Patterns and controls of light use efficiency in four contrasting forest ecosystems in Yunnan, Southwest China

Xue-Hai Fei[1, 2, 3], Qing-Hai Song[1, 3]*, Yi-Ping Zhang[1, 3]*, Gui-Rui Yu[4], Lei-Ming Zhang[4], Li-Qing Sha[1, 3], Yun-Tong Liu[1, 3], Kun Xu[5], Hui Chen[1, 6], Chuan-Sheng Wu[7], Ai-Guo Chen[1, 8], Shu-Bin Zhang[1, 8], Wei-Wei Liu[5], Hua Huang[5], Yun Deng[1, 6], Hai-Lang Qin[1, 6], Pei-Guang Li[9], John Grace[10]

1. CAS Key Laboratory of Tropical Forest Ecology, Xishuangbanna Tropical Botanical Garden, Chinese Academy of Sciences, Menglun, Yunnan 666303, China
2. College of Resource and Environmental Engineering, Guizhou University, Guiyang 550025, China
3. Global Change Ecology Group, Xishuangbanna Tropical Botanical Garden, Chinese Academy of Sciences, Menglun 666303, China
4. Synthesis Research Center of Chinese Ecosystem Research Network, Key Laboratory of Ecosystem Network Observation and Modeling, Institute of Geographic Sciences and Natural Resources Research, Chinese Academy of Sciences, Beijing 100101, China
5. Lijiang Forest Ecosystem Research Station, Kunming Institute of Botany, Chinese Academy of Sciences, 132# Lanhei Road, Heilongtan, Kunming 650201, Yunnan, China
6. Xishuangbanna Station for Tropical Rainforest Ecosystem Studies, Menglun, Xishuangbanna, Yunnan 666303, China
7. Anhui Province Key Laboratory of Embryo Development and Reproductive Regulation, Anhui Province Key Laboratory of Environmental Hormone and Reproduction, Fuyang Normal University, Fuyang, Anhui Province, 236037, China
8. Yuanjiang Savanna Ecosystem Research Station, Xishuangbanna Tropical Botanical Garden, Chinese Academy of Sciences, Yuanjiang, Yunnan 653300, China
9. Yellow River Delta Ecological Research Station of Coastal Wetland, Yantai Institute of coastal Zone Research, Chinese Academy of Sciences, Yantai 264003, China
10. School of GeoSciences, the University of Edinburgh, Edinburgh EH9 3JN, UK

This article has been accepted for publication and undergone full peer review but has not been through the copyediting, typesetting, pagination and proofreading process which may lead to differences between this version and the Version of Record. Please cite this article as doi: 10.1029/2018JG004487

*Corresponding authors: Yi-Ping Zhang (yipingzh@xtbg.ac.cn) and Qing-Hai Song (sqh@xtbg.ac.cn).

Tel.: +86-871-65160904; Fax: +86-871-65160916

Corresponding author address: Xishuangbanna Tropical Botanical Garden, Chinese Academy of Sciences

88 Xuefu Road, Kunming, Yunnan, P.R. China

Postal code: 650223

Running title: Forest ecosystem light use efficiency

Key Points:

1 Evergreen broad-leaved forest (EBF) ecosystem shows higher LUE than subalpine coniferous/savanna ecosystems.

2 Ecosystems with similar/same forest type show nearly the same LUE despite considerable spatiotemporal variability in LUE.

3 The vapor pressure deficit (VPD) and leaf area index (LAI) largely determine the variability in LUE.

4 Warming might decrease LUE in the savanna ecosystem and may increase LUE in the other three ecosystems.

Abstract

Ecosystem light use efficiency (LUE) is a critical parameter in estimating CO_2 uptake by vegetation from climatological and satellite data. However, the spatiotemporal dynamics and biophysical regulations of ecosystem-level LUE are not well understood, resulting in large uncertainties in the estimation of gross primary productivity (GPP) using LUE-based models. In this study, we used eddy covariance (EC) to explore spatiotemporal variations and controls of LUE in four contrasting forest ecosystems (savanna, tropical rainforest, subtropical evergreen forest, and subalpine coniferous forest). Based on 27 site-years of data, we found that 1) the multiyear mean LUE was 0.063, 0.251, 0.247, and 0.140 g C · mol photon^{-1} in the four contrasting ecosystems; 2) the LUE in the wet season (May-October) was higher than that in the dry season in all studied ecosystems; 3) the leaf area index (LAI) controlled GPP and LUE significantly and explained 74%, 29%, 54%, and 36% of the variation in GPP and 51%, 19%, 41%, and 54% of the variation in LUE in the four contrasting ecosystems; 4) path analysis revealed the critical roles of GPP and vapor pressure deficit (VPD) in controlling LUE in these four forest ecosystems; and 5) under warming scenarios, LUE may decrease in savanna but increase in the other three ecosystems, while decreasing precipitation (P) may reduce LUE in the ecosystems studied. This study improves our understanding of the influence of biophysical factors on LUE and demonstrates how LUE changes with variations in temperature, soil moisture and LAI, thereby improving estimations of large-scale carbon exchange/cycling.

Keywords: Ecosystem light use efficiency, Critical factors, Path analysis, Climate change, Forest ecosystems, Eddy covariance

1 Introduction

Light use efficiency (LUE) was historically defined as the ratio of the total or aboveground net primary production (NPP, or ANPP), or sometimes the gross primary production (GPP), to the incident photosynthetically active radiation (PAR) [*Austin et al.*, 1978; *Nichol et al.*, 2000; *Pangle et al.*, 2009], absorbed PAR (APAR) [*Monteith*, 1972; *Xiao et al.*, 2004a] or APAR for green leaves [*Hall et al.*, 1992; *Gitelson and Gamon*, 2015]. LUE is a characterization of the sensitivity of photosynthetic productivity to incoming solar irradiation, temperature and water conditions [*Gilmanov et al.*, 2007; *Shi et al.*, 2014]; thus, LUE is a critical trait of ecosystems and is the underlying basis for estimating carbon exchange in many existing scale-up models (e.g., CASA [*Potter et al.*, 1993], GLO-PEM [*Prince and Goward*, 1995], MODIS GPP [*Running et al.*, 2004; *Zhao et al.*, 2005], VPM [*Xiao et al.*, 2004a; *He et al.*, 2014] and EC-LUE [*Alton et al.*, 2007; *Yuan et al.*, 2007; *Li et al.*, 2008; *Mercado et al.*, 2009; *Zhou et al.*, 2016]). All

of these models rely on *a priori* estimates of LUE. Therefore, an understanding of LUE and its controls is usually necessary for studies on spatiotemporal variations in the global carbon cycle [*Zhao et al.*, 2007].

Conceptually, there are two categories of LUE. The first is physiological LUE (LUE_{phys} = GPP/APAR), which is widely applied in MODIS-based models to model regional/global GPP [*Running et al.*, 2004; *Zhao et al.*, 2007; *Tang et al.*, 2015; *Zhou et al.*, 2016], in studies at the leaf, individual, population, and community levels (especially at the canopy scale) [*Larcher*, 2003] and in characterizations of physiological–biochemical parameters [*Gilmanov et al.*, 2010]. The second category is ecological LUE (LUE_{eco} = GPP/PAR), which is used in studies at the ecosystem level and is mainly applied in EC-based models to scale GPP up to the biome/regional level [*Cooper*, 1970; *Odum and Barrett*, 1971; *Austin et al.*, 1978; *Gilmanov et al.*, 2007; *Gilmanov et al.*, 2010; *Shi et al.*, 2014; *Zhang et al.*, 2015a]. In the present report, we focus on LUE at the ecosystem level. Therefore, the second definition of LUE (i.e., ecosystem light use efficiency, LUE_{eco}) was employed in this study as LUE_{eco} (hereafter LUE, with units in g C · mol photon^{-1}), not only reflecting the ecophysiological properties of vegetation but also taking into account certain additional ecosystem-level characteristics (such as plant properties, aboveground biomass, and leaf area index (LAI)) [*Gilmanov et al.*, 2007].

Traditionally, the biomass inventory approach has been applied to study LUE, where the uptake of carbon is the increase in biomass, similar but not identical to the NPP [*Cannell et al.*, 1987]. New techniques, including the eddy covariance (EC)-based method [*Ruimy et al.*, 1995; *Yuan et al.*, 2007; *Li et al.*, 2008] and model inversions based on EC or GIS [*Garbulsky et al.*, 2010; *Tang et al.*, 2015; *Yebra et al.*, 2015], are currently applied in the study of LUE. EC-based LUE is broadly used because ecosystem-scale GPP can be estimated with good accuracy based on EC [*Baldocchi*, 2003] and because EC is widely used globally. In addition, at the ecosystem scale, EC-based LUE at well-instrumented sites provides important supplementary data for revealing the spatiotemporal characteristics and driving factors of LUE [*Garbulsky et al.*, 2010; *Gilmanov et al.*, 2010; *Zhang et al.*, 2015a].

The combined effects of vegetation properties and climate (such as species composition, carboxylase activity/density, leaf nitrogen or phosphorus content, LAI, biomass, PAR, temperature (T), precipitation (P), and CO_2 concentrations) result in obvious spatiotemporal variations in LUE [*Green et al.*, 2003; *Still et al.*, 2004; *Tong et al.*, 2009]. Previous studies have reported that LUE is mainly limited by temperature and soil moisture [*Traore et al.*, 2014] as well as LAI through its modulation of canopy-scale photosynthesis *Eamus et al.* [2001]. An analysis of a dataset containing 21 ecosystems concluded that rainfall was the key factor

affecting LUE [*Kanniah et al.*, 2011]. Therefore, studies on the spatial patterns and temporal dynamics of ecosystem LUE and the controlling factors thereof are necessary for understanding and predicting the carbon cycle and energy fixation [*Gilmanov et al.*, 2007; *Zhao et al.*, 2007; *Zhang et al.*, 2015b]. However, the spatiotemporal variations in LUE and its controls remain poorly documented in many regions.

Yunnan Province, which is located in southwest China, is famous for its high biodiversity and has been called a "biodiversity kingdom" [*Wu et al.*, 1987] due to its location and altitudinal variation (a difference of 6664 m from south to north), which result in a climatic gradient. Additionally, almost all types of ecosystems (e.g., tropical/savanna/subtropical/temperate forest, alpine meadow, and tundra) can be found in Yunnan [*Wu et al.*, 1987]. Furthermore, southwest China (including Yunan, Guizhou, and Sichuan) has the largest forest carbon storage [*Tang et al.*, 2018] and highest carbon sink rate [*Piao et al.*, 2009]. However, to the best of our knowledge, there are no studies on LUE and its controlling factors at the ecosystem scale. Therefore, we conducted an EC-based assessment of LUE in four contrasting forest ecosystems (the Yuanjiang savanna ecosystem (YJ), Xishuangbanna tropical rainforest ecosystem (XSBN), Ailaoshan subtropical evergreen broad-leaved forest ecosystem (ALS) and Lijiang subalpine coniferous forest ecosystem (LJ)) in Yunnan with the following specific objectives: 1) to investigate LUE and its spatiotemporal dynamics between/within contrasting forest ecosystems; 2) to acquire the LUE_{max} value for calibrating and validating LUE-based models; and 3) to quantify the contributions of critical factors on LUE and its responses to LAI, T, and P. These objectives will contribute to a better understanding of the effects of critical controls on ecosystem LUE and validate LUE-based models for estimating biome/regional GPP and even global carbon cycling.

2 Materials and Methods

2.1 Site information

Four representative forest ecosystems (YJ, XSBN, ALS, and LJ) (Figure 1) were chosen several years ago and fully instrumented to enable state-of-the-art measurements of CO_2 fluxes. The work reported here is part of that larger investigation. The climate in this region is mainly influenced by the southwest monsoon and by the Tibetan Plateau in each of the four locations. The mean annual temperature (MAT) during the study period in YJ, XSBN, ALS, and LJ was 24.3, 21.4, 11.7, and 7.9°C, and the mean annual precipitation (MAP) was 734, 1415, 1728, and 1095 mm, respectively (Figure 1, Table 1), with more than 77% of the MAP occurring during the wet season (May-October) (Table 1). The geographical location, elevation, biophysical controls, dominant species, and soil physicochemical properties are listed in Table 1, and

further information about the topography, climate, solar radiation, vegetation, and soil properties of this region can be found in previous studies [*Cao et al.*, 2006; *Fei et al.*, 2017; *Huang et al.*, 2017; *Song et al.*, 2017; *Fei et al.*, 2018].

2.2 Eddy covariance-based LUE

2.2.1 Flux, meteorological and LAI data

An open-path eddy covariance (OPEC) system, which directly provides a high time-resolution dataset on energy/carbon/H_2O flux between the ecosystem and atmosphere [*Baldocchi et al.*, 1996; *Aubinet et al.*, 2001; *Baldocchi et al.*, 2001], and a routine meteorological observing system (RMOS) were applied to measure climatic variables simultaneously in all four of these ecosystems beginning in May 2013, October 2002, September 2008, and August 2014 in YJ, XSBN, ALS and LJ, respectively. Details about the four sets of OPEC and RMOS used in the present research are provided in Table 2. The flux and meteorological data sampling frequencies were 10 Hz and 0.5 Hz, respectively. All data were continuously collected using Campbell loggers (CR1000/CR3000/CR5000, Campbell Scientific Inc., Logan, UT, USA). A LAI-2200 plant canopy analyzer (Li-Cor Inc., USA) was used to measure the monthly LAI at the end of each month (8 plots × 4 repeats), and data were processed with FV2200 software (Li-Cor Inc., USA). Data from the following periods were used in the present study: May 2013 to 2016, 2003 to 2016, 2009 to 2014, and August 2014 to 2016 in YJ, XSBN, ALS, and LJ, respectively. All the data shown in tables/figures are multi-day/month/year averaged values.

2.2.2 Flux data processing, filling and partitioning

Quality assessment and control (QA/QC), including coordinate rotation [*Tanner and Thurtell*, 1969; *Wilczak et al.*, 2001], WPL calibration [*Webb et al.*, 1980; *Lee and Massman*, 2010], storage flux calculation [*Hollinger et al.*, 1994; *Baldocchi et al.*, 1996], outliers exclusion [*Yu et al.*, 2006] and u* filtering [*Reichstein et al.*, 2005], were applied to control and ensure the quality of flux data. In addition, the flux data gaps were filled, and the data were partitioned according to the FLUXNET/CarboEurope methodology [*Falge et al.*, 2001; *Reichstein et al.*, 2005] to obtain robust GPP data. The details of the flux data QA/QC and post-processing procedures used in this study are described in *Reichstein et al.* [2005] and *Yu et al.* [2006].

2.2.3 Ecosystem LUE calculation

Ecosystem light use efficiency (LUE) was defined as the ratio of gross primary productivity (GPP) to total incident photosynthetically active radiation (PAR) [*Austin et al.*, 1978; *Gilmanov et al.*, 2007], as expressed in Equation (1):

$$\mathrm{LUE} = \frac{\mathrm{GPP}}{\mathrm{PAR}} \quad (1)$$

where the units of GPP, PAR, and LUE are μg C m^{-2} s^{-1}, μmol photon m^{-2} s^{-1}, and g C • mol $photon^{-1}$, respectively. PAR was measured directly with the LQS70-10 sensor (Table 2), and GPP was derived from the eddy flux [*Baldocchi et al.*, 2001; *Reichstein et al.*, 2005; *Yu et al.*, 2006; *Gilmanov et al.*, 2007], as expressed in Equations (2), (3), and (4):

$$\mathrm{GPP} = \mathrm{R}_{eco} + (-\mathrm{NEE}) \quad (2)$$

$$\mathrm{NEE} = \mathrm{F_c} + \mathrm{F_s} = \rho\overline{w'c'} + \frac{\Delta c}{\Delta t} z_r \quad (3)$$

$$\mathrm{R}_{eco} = \mathrm{R}_{eco,\ ref} \times e^{E_0 \left(\frac{1}{T_{ref} - T_0} - \frac{1}{T - T_0}\right)} \quad (4)$$

where NEE is the net ecosystem carbon exchange and consists of the turbulent eddy flux (F_c) and storage flux (F_s) [*Hollinger et al.*, 1994; *Baldocchi et al.*, 1996; *Aubinet et al.*, 2001; *Lee et al.*, 2006]; ρ, w, and c represent the air density, vertical wind velocity, and target scalar concentration (CO_2 concentration in this case), respectively. The primes denote fluctuations from the average, and the overbar signifies a time average (30 min in this study). Δc is the variation over a 30-min period at height z_r, z_r is the height of the EC system (13.9, 48.8, 34.0, and 60.0 m in YJ, XSBN, ALS, and LJ, respectively), and Δt is the time interval (1800 s in this case). R_{eco} is the ecosystem respiration and is calculated according to *Lloyd and Taylor* [1994]; $R_{eco,\ ref}$ is the reference ecosystem respiration at a reference temperature (T_{ref}; here, 10°C is used); $R_{eco,\ ref}$ and E_0 are the fitted parameters; T_0 is a constant and is set to 227.13 K (–46.02°C); and T is the measured 5-cm soil temperature in the present study. Note that T_0, T_{ref}, and T in Equation (4) are in Kelvin (degK).

2.3 Statistical analysis

2.3.1 Path analysis

In the present study, we applied path analysis [*Wright*, 1921] to explore which biophysical controls impact LUE significantly and to suggest the relative importance of these controls by parameterizing the standardized direct and total effects on LUE at a monthly timescale due to the effects of climatic factors on GPP [*Reichstein et al.*, 2007; *Baldocchi*, 2008; *Yu et al.*, 2013a; *Baldocchi et al.*, 2018]. We designed the

path structure for the correlations of global radiation (R_g), air temperature (T_{air}), vapor pressure deficit (VPD), relative humidity (RH), precipitation (P), soil volumetric water content (SVWC), GPP and PAR as follows: 1) PAR and SVWC influence GPP directly, while T_{air} and P determine GPP directly and indirectly; 2) R_g influences PAR and T_{air} directly, P influences RH and SVWC directly, and T_{air} and RH determine VPD jointly; and 3) R_g, T_{air}, VPD, RH, P, SVWC, GPP and PAR determine LUE directly and indirectly.

Path analysis is based on the fundamental principles of multiple regression and correlation analysis but has a more interpretive structure [*Grace and Bollen*, 2005]. It reveals not only the direct effects of independent factors on dependent variables but also the indirect and total effects [*Li*, 1975; *Schemske and Horvitz*, 1988; *Wootton*, 1994]. The R package *sem* [*Fox et al.*, 2016] was used to perform the path analysis, and the path coefficients (PCs) were standardized partial regression coefficients representing the relative strength of a given relationship and allowed us to quantitatively compare the relative influences of R_g, T_{air}, VPD, RH, P, SVWC, GPP and PAR on LUE.

2.3.2 Regression analysis

We used the following one-factor linear/quadratic regression model (Equations (5) and (6)) to explore the responses of ecosystem LUE to T_{air} and SVWC at daily timescales:

$$LUE = ax + b \quad (5)$$

$$LUE = ax^2 + bx + c \quad (6)$$

where a, b, and c are fitted parameters; x represents T_{air} or SVWC in this research.

3 Results

3.1 Ecosystem LUE

3.1.1 Diurnal patterns in GPP, PAR, and LUE

We analyzed the seasonally and yearly binned daytime (PAR>50 μmol m^{-2} s^{-1}) patterns of GPP, PAR, and LUE and found "U" patterns of daytime courses of GPP, PAR, and LUE in all four ecosystems (YJ, XSBN, ALS, and LJ) (Figure 2). GPP increased with increasing PAR (after sunrise), peaked midday between 12:00-14:00 and then decreased with decreasing PAR values (after midday), whereas LUE showed the opposite diurnal trends and reached a minimum at midday, even though the maximum GPP remained stable during this period (Figure 2). LUE values were larger and ecosystems were more photosynthetically efficient at sunrise/sunset, while GPP values were lower for the lower PAR. Therefore, photosynthetic productivity (namely, GPP) was limited by lack of PAR in the early morning and at dusk.

LUE was very high at XSBN and ALS (>0.50 g C · mol photon^{-1}) compared with YJ (<0.16 g C · mol photon^{-1}), and the order of LUE diurnal amplitude was XSBN>ALS>LJ>YJ as a result of GPP showing the same general pattern. At the same time, the order of the diurnal amplitude of PAR was YJ>XSBN>LJ>ALS (Figure 2). These findings suggest that the broad-leaved forest ecosystems (e.g., XSBN and ALS) show higher photosynthetic efficiency than coniferous/savanna forest ecosystem (e.g., LJ and YJ, respectively) and the lower altitude is usually associated with a larger annual PAR.

3.1.2 Ranges of annual LUE and LUE_{max} values

Multiyear daily LUE values ranged from 0.008-0.316, 0.065-1.073, 0.060-1.129, and 0.052-0.881 g C · mol photon^{-1} in YJ, XSBN, ALS, and LJ, respectively (Figure 3). We analyzed the eight-day average LUE_{max} at an annual time scale to reduce the uncertainty caused by noise-data, and many MODIS-based GPP estimations are produced at this timescale. The multiyear eight-day average LUE_{max} values were 0.171, 0.539, 0.708, and 0.480 g C · mol photon^{-1} in YJ, XSBN, ALS, and LJ, respectively (Table 3). These results suggest that ALS (evergreen broad-leaved forest) exhibits the highest photosynthetic capability, whereas the LUE_{max} in YJ (savanna) is the lowest and is severely constrained by biophysical factors compared to the other three ecosystems.

3.1.3 Intra-annual dynamics of the controls and LUE

The variation in climatic factors and LUE showed the following: 1) R_g and PAR peaked from April to May in each of the forest ecosystems. The dynamics of PAR were highly coincident with R_g in the same ecosystems, whereas R_g and PAR changed dramatically in the wet season in ALS and LJ compared with YJ (Figure 4a, e). 2) The lowest T_{air} occurred from the end of December to the middle of January, and the highest T_{air} was observed in May to June in YJ but in July in XSBN, ALS, and LJ (Figure 4b). Generally, VPD decreased with the onset of the rainy season in the four ecosystems. The multiyear mean VPD values were 13.7, 6.3, 3.4, and 3.6 hPa in YJ, XSBN, ALS, and LJ, respectively, and VPD was found to change dramatically in YJ, peaking from April to May (Figure 4b). 3) The SVWC at –5 cm changed consistently in the four ecosystems. The lowest SVWC occurred at the end of the dry season (April), and the SVWC was higher in the wet season (Figure 4d) because more than 77% of precipitation falls during the rainy season (Figure 4c, Table 1) and variations in SVWC are highly coupled with precipitation dynamics (Figure 4c). 4) According to the multiyear daily mean LUE results, the highest daily mean values of LUE (g C · mol photon^{-1}) were 0.196 (DOY 232), 0.448 (DOY 180), 0.630 (DOY 179), and 0.479 (DOY 199) in

YJ, XSBN, ALS, and LJ, respectively. Additionally, the lowest GPP and the highest PAR resulted in the lowest LUE in YJ, and the daily LUE in this area was much lower than that in the other three forest ecosystems (Figure 4d, e, f). 5) Both GPP and PAR exhibited strong daily, seasonal, and spatial/inter-site variability (Figure 4d, e) that contributed to dramatic spatiotemporal variations in LUE. Though LUE showed large daily variability, we can clearly see that LUE during May-October (DOY121-305) was higher than that in the other periods (Figure 4f). Overall, the 4 forest ecosystems showed large fluctuations in the daily magnitude of LUE within the same ecosystem and clear spatial variations in LUE among YJ, XSBN, ALS and LJ.

3.1.4 Monthly variation in LUE

All monthly LUE values in LJ were lower than the corresponding monthly LUE in XSBN and ALS. Similar monthly LUE variations were found in YJ, where the monthly LUE values were lower than the corresponding monthly LUE in XSBN, ALS and LJ (Figure 5a), which had the lowest monthly LAI (Figure 5b) and the highest monthly VPD (Figure S1) . Furthermore, even the highest monthly LUE (in August) in YJ was lower than the lowest monthly LUE (in February) both in XSBN and ALS (Figure 5a). This finding indicates that the YJ savanna ecosystem exhibited much lower LUE than that found in the other studied forest ecosystems.

From June to November, the monthly LUE values in ALS were higher than those in XSBN, whereas the rest of the monthly LUE values in ALS were lower than those in XSBN (Figure 5a). The lowest monthly LUE was observed in March (0.037 g C · mol photon^{-1}), February (0.162 g C · mol photon^{-1}), February (0.113 g C · mol photon^{-1}), and January (0.082 g C · mol photon^{-1}) in YJ, XSBN, ALS, and LJ, respectively. The highest monthly LUE occurred in August (0.119 g C · mol photon^{-1}) in YJ and in July (0.350, 0.495, 0.294 g C · mol photon^{-1}) in XSBN, ALS, and LJ, although the highest monthly LAI values were observed in August (Figure 5b).

3.1.5 Seasonal and annual patterns in meteorological factors and LUE

The R_g, PAR, P, T_{air}, RH, and SVWC were higher during the wet season than during the dry season except for the R_g and PAR in ALS and LJ (Table 4). The VPD in XSBN, ALS, and LJ was typically larger during the dry season than during the wet season because nearly 80% of the annual precipitation fell during the wet season. However, in YJ, VPD showed the opposite seasonal trend and was 15.2 hPa during the wet

season and 12.1 hPa during the dry season (Table 4) due to abundance of R_g and higher temperature in the wet season (Figure 4).

Generally, the magnitude of LUE in these typical forest ecosystems in Yunnan exhibited the order XSBN>ALS>LJ>YJ regardless of whether it was examined only during the dry season, only during the wet season, or for the whole year, except the LUE in ALS in the wet season was greater than that in XSBN. The LUE in YJ was the lowest regardless of whether examining only the dry season, only the wet season, or the entire year was compared with XSBN, ALS, and LJ, and a lower LUE was observed in LJ than in XSBN and ALS. In addition, the seasonal and annual patterns of LUE in each of the 4 ecosystems showed a clear trend of wet season>annual>dry season. The LUE values were 0.044, 0.213, 0.160, and 0.098 g C · mol photon^{-1} in the dry season; 0.078, 0.290, 0.351, and 0.193 g C · mol photon^{-1} in the wet season; and 0.063, 0.251, 0.247 and 0.140 g C · mol photon^{-1} annually in YJ, XSBN, ALS, and LJ, respectively (Figure 6).

3.2 Quantifying the contributions of critical factors to LUE

Results of the path analysis show a network of influences. To further quantify how critical controls influenced the LUE, we applied a path analysis to quantitatively compare the direct and total effects of R_g, P, T_{air}, RH, SVWC, VPD, PAR and GPP on LUE (Figure 7). Specifically, we found that the critical factors affecting LUE were as follows: 1) in YJ, the critical factors were GPP, P, RH, VPD and PAR, and the standardized total effects (STE) were 0.96, 0.66, 0.60, –0.47, and –0.45, respectively. This finding suggests that higher VPD/PAR values have negative effects on LUE in YJ. 2) In XSBN, the critical factors were GPP, P, VPD, T_{air} and PAR with STEs of 0.93, 0.52, –0.33, 0.34, and –0.43, respectively. 3) In ALS, the critical factors were GPP, VPD, and T_{air} with STEs of 0.81, –0.58, and 0.45, respectively. 4) In LJ, the critical factors were GPP, P, VPD, T_{air}, and PAR with STEs of 0.77, 0.32, –0.70, 0.35, and –0.31, respectively. The results showed that LUE values in LJ and ALS were more sensitive to VPD than in YJ and XSBN. Overall, LUE showed a negative relationship with R_g, VPD, and PAR and a positive relationship with other factors (P, T_{air}, RH, SVWC and GPP). Furthermore, LUE values were mainly controlled by GPP, which exhibited STEs of 0.96, 0.93, 0.81 and 0.77 on LUE in YJ, XSBN, ALS and LJ, respectively (Figure 7). Therefore, the variations in LUE were mainly controlled by variations in GPP, P, T_{air}, VPD and PAR although with different path coefficients in different ecosystems. In summary, GPP and VPD play especially critical roles in controlling LUE in the 4 studied forest ecosystems.

3.3 Relationship between GPP and PAR

We used a quadratic model to explore the light response of GPP and found that GPP increased first with increasing PAR and then decreased when PAR reached a certain threshold in YJ, XSBN, and ALS (the threshold was 1543, 1440, and 1113 μmol m^{-2} s^{-1}, respectively) (Figure 8a, b, c), but a different pattern (the higher PAR, the larger the GPP) was observed in LJ (Figure 8d). Furthermore, GPP in ALS reached the maximum first with the increasing PAR and then in XSBN and in YJ. Thus, photoinhibition did not occur in LJ, while it did occur in the other three forest ecosystems. This finding revealed that the lack of PAR constrained GPP in LJ.

3.4 Responses of GPP and LUE to LAI

Based on the linear regression analysis, we found that the sensitivity of GPP to LAI was YJ>ALS>LJ>XSBN (R^2 values were 0.74, 0.54, 0.36, and 0.29, respectively). LUE showed the highest sensitivity to LAI in LJ and YJ, whereas the lowest sensitivity was observed in XSBN (Figure 9a-d). This result suggested that LAI exerts more influence on GPP and LUE in savanna ecosystems (e.g., YJ) than in tropical forest ecosystems (e.g., XSBN). Overall, LAI showed highly significant influences on GPP and LUE not only in each of the four forest ecosystems (Figure 9 a-d) but also in the studied forest ecosystems as a whole (Figure 9e).

3.5 Responses of LUE to temperature and soil moisture

Generally, LUE increased with increasing temperatures in XSBN, ALS, and LJ, although the rate of increase in LUE was in the order XSBN<LJ<ALS according to the quadratic regression results (Figure 10b, c, d). However, a different temperature response pattern was observed in YJ in which LUE increased first when temperature was lower than ~26.5°C and then decreased with increasing temperature (Figure 10a). Compared with the relationship between temperature and LUE, the relationship between SVWC and LUE was simple and coherent, exhibiting a trend in which LUE increased with increasing SVWC (Figure 11). Meanwhile, LUE increased dramatically in XSBN and ALS (Figure 11b, c). In summary, LUE showed positive relationships with temperature and soil moisture in all of the studied forest ecosystems except in YJ, where LUE decreased with temperatures >26.5°C. These findings revealed that a decrease in precipitation will decrease the LUE of forest ecosystems, whereas warming might increase the LUE in other ecosystems along with a decrease in the water-shortage area (e.g., arid/semiarid/savanna ecosystem).

4 Discussion

4.1 The spatiotemporal variability/dynamics of LUE

Understanding the spatial patterns and temporal dynamics of LUE is of great interest for estimating photosynthetic productivity and for studying the carbon cycle [*Zhao et al.*, 2007; *Zhang et al.*, 2015b]. In the present study, we found that with respect to the temporal dynamics of LUE, the multiyear mean daily maximum LUE (LUE_{max}) was 0.196 (DOY 232), 0.448 (DOY 180), 0.630 (DOY 179), and 0.479 (DOY 199) g C · mol photon^{-1} in YJ, XSBN, ALS, and LJ, respectively (Figure 4f), which suggests that LUE_{max} occurred in the early-to-mid wet season and shows that favorable water and temperature conditions are helpful in increasing LUE. A general pattern was observed in which the LUE values in all four of the forest ecosystems studied here (Figure 1) increased consistently until the middle of the wet season (in July/August) and then decreased (Figure 5a). Consequently, the LUE values in the wet season were greater than those in the dry season in XSBN and ALS (i.e., evergreen broad-leaved forest (EBF)), in LJ (i.e., evergreen needle-leaved forest (ENF)), and in YJ (i.e., savanna) because nearly 80% of the precipitation falls during this period (Table 4, Figure 4c) and higher GPP occurs in the wet season (Figure 4d). Previous studies found a similar trend in which the wet season had higher GPP and LUE values than the dry season [*Gilmanov et al.*, 2007; *Shi et al.*, 2014; *Zhang et al.*, 2015a]. Interestingly, the highest monthly LUE values in XSBN, ALS, and LJ were all observed in July, but there was a delay in YJ, where this highest value occurred in August (Figure 5a) although the monthly LAI_{max} was reached in August in all four ecosystems (Figure 5b).However, YJ had the highest temperatures and VPD throughout the year compared with the other three ecosystems (Table 4, Figure 4b). Therefore, we thought that variation in monthly VPD (Figure S1) caused the highest monthly LUE value to delay to August in YJ.

With regard to the spatial variation of LUE, we observed that the multiyear mean annual LUE values were 0.063, 0.251, 0.247, and 0.140 g C · mol photon^{-1} in YJ, XSBN, ALS, and LJ, respectively, which indicates that EBF ecosystems (e.g., XSBN and ALS) are more light efficient (i.e., exhibit higher LUEs) than coniferous forest ecosystems (e.g., LJ). Our results reveal that the savanna ecosystem (e.g., YJ) shows the lowest LUE compared with the former two categories of forest ecosystems (Figure 5a, Figure 6) regardless of whether examining only the dry/wet season or the annual value (Figure 6). Although our findings are contrary to those from a study in Canada, where LUE in grassland was found to be higher than in forest [*Schwalm et al.*, 2006], our results agree well with most previous findings indicating that EBF has the highest LUE [*Shi et al.*, 2014; *Yuan et al.*, 2014; *Jia et al.*, 2016], followed by ENF [*Wei and Wang*, 2010].

The multiyear mean eight-day binned LUE_{max} (0.480 g C · mol photon^{-1}) in LJ (Table 3) was only slightly higher than three-year mean eight-day binned LUE_{max} (0.476 g C · mol photon^{-1}) in a broad-leaved Korean mixed pine forest [*Zhang et al.*, 2015a], although the distance between these sites is greater than 3500 km. This trend was also observed in XSBN and ALS (both of which are EBF, where the multiyear mean LUE was 0.251 and 0.247 g C · mol photon^{-1}, respectively (Figure 6)). These findings indicate that ecosystems with a similar forest type may have similar LUEs. In summary, ecosystems with similar/same forest/vegetation type show nearly the same LUE despite considerable spatiotemporal variability, demonstrating that it is possible and reliable to upscale site-based LUE to predict regional/global GPP.

4.2 Reponses of GPP to PAR and LAI

The critical factors driving GPP should be explored as GPP and LUE are closely related (Figure 7). We mainly focus on PAR and LAI in this study because both factors not only influence GPP but also influence LUE directly and significantly [*Zhao et al.*, 2007; *Shi et al.*, 2014]. We found that with increasing PAR, GPP first increases and then decreases when PAR exceeds a certain threshold in YJ, XSBN and ALS (Figure 8). This finding is consistent with previously published results [*Turner et al.*, 2003; *Gilmanov et al.*, 2007; *Mercado et al.*, 2009]. Similar to other results reported for a mixed forest [*Zhang et al.*, 2015a], GPP was linearly correlated with PAR in LJ, meaning that a higher PAR did not saturate photosynthesis (Figure 8d) and that a decreased PAR in the wet season may inhibit photosynthesis (Figure 4e4). These findings indicate that slightly increasing PAR (i.e., a little less rainy/cloudy days) in the wet season might enhance the GPP in LJ. Compared with the responses of GPP to PAR, there is clear evidence that GPP increases continuously with increasing LAI [*Li et al.*, 2008; *Wang et al.*, 2008; *Gilmanov et al.*, 2010]. Our results show that LAI plays a key positive role in forest photosynthesis (Figure 9a), although LAI shows less of an influence on GPP in XSBN (tropical forest), where LAI explained nearly 30% in of the variation in GPP (Figure 9b1). However, LAI explained 74% of the variation in GPP in YJ (savanna) (Figure 9a1). This finding indicates that the higher the LAI is, the higher the GPP. Therefore, LAI should be considered seriously when estimating/upscaling regional GPP based on the LUE model.

4.3 Influences of biophysical factors on LUE

Theoretically, and under ideal conditions, the assimilation of 1 mol of CO_2 requires 8 moles of photons [*Xiao*, 2006] at the leaf scale, which means that the leaf-scale theoretical maximum LUE_{max} is 1.5 g C · mol photon^{-1}. Thus, the ecosystem-scale LUE_{max} should be higher than 1.5 g C · mol photon^{-1}. However, the measured LUE values were much lower than the theoretical LUE_{max} because LUE is constrained by

many biophysical factors, such as the community structure, biomass, carboxylase density, nutrition content in soil/leaf, LAI, PAR, T, water, CO_2 concentration, VPD, spectral composition and stomatal conductance [*Green et al.*, 2003; *Still et al.*, 2004; *Zhao et al.*, 2007]. In this study, the daily LUE values ranged from 0.008-0.316, 0.065-1.073, 0.060-1.129, and 0.052-0.881 g C · mol photon^{-1} in YJ, XSBN, ALS, and LJ, respectively (Figure 3). The highest eight-day binned LUE_{max} was 0.827 g C · mol photon^{-1} in ALS (Table 3), and the values in the middle of the wet season were much lower than the theoretical LUE_{max} (1.5 g C · mol photon^{-1}). Therefore, it is necessary to explore the critical factors that determine the variations in LUE. Increasing P/SVWC leads to decreased VPD [*Zhao et al.*, 2007], which increases GPP by enhancing canopy stomatal conductance [*Beer et al.*, 2009] and results in increased CO_2 and H_2O exchanges. As a result, LUE is enhanced when P/SVWC increases and when VPD decreases.

In the present study, the path analysis results revealed that LUE has a positive relationship with P, T_{air}, RH, SVWC and GPP and a negative relationship with R_g, VPD, and PAR (Figure 7, Figure 10, Figure 11). These results agree well with those of previously published studies [*Zhao et al.*, 2007; *Beer et al.*, 2009; *Shi et al.*, 2014; *Zhang et al.*, 2015a]. Specifically, P is a strong determinant of GPP and, hence, LUE in the savanna ecosystem (YJ) (Figure 7), and this finding is consistent with previous studies [*Li et al.*, 2008; *Shi et al.*, 2014], while T shows more influence on GPP and LUE in the subtropical evergreen broad-leaved forest ecosystem (ALS) (Figure 7), which has a high MAP and a lower MAT (Table 1, Table 4). In addition, P plays a key role in LUE in YJ and XSBN, which have a higher MAT than that found in ALS and LJ (Table 4). This dynamic indicates that water availability constrains LUE in hot and dry areas. In contrast, T is more important in determining LUE than P in ALS and LJ (Figure 7), where the MAT is lower (Table 4), suggesting that T is the determinant in cold/high elevation areas. LUE shows a strong positive relationship with LAI in which LUE increases strongly with increasing LAI (Figure 9, Figure S2). This trend of a strong control of LUE by LAI has also been found in other studies [*Eamus et al.*, 2001; *Shi et al.*, 2014; *Zhang et al.*, 2015a]. Some studies have shown that LUE is mainly controlled by T and soil moisture [*Xiao et al.*, 2004b; *Traore et al.*, 2014] or P [*Li et al.*, 2008; *Kanniah et al.*, 2011]. In summary, T, P, VPD, LAI, PAR, and GPP are the primary determinants (especially GPP, VPD, and LAI) of LUE, although the magnitudes of each influence are not exactly the same among the four studied forest ecosystems (YJ, XSBN, ALS, and LJ) on a monthly time scale (Figure 7, Figure 9). The regression analysis revealed that LUE increased with increasing T_{air} and SVWC in all of the forest ecosystems except for YJ (savanna), where LUE decreased when T_{air} exceeded approximately 26.5°C, which indicated that LUE will decrease

in YJ but might increase in XSBN, ALS, and LJ under warming scenarios. Therefore, the changing climate (warming/decreasing precipitation) will decrease the LUE and GPP in arid/semiarid regions.

5. Implications and Conclusions

Based on the 27 site-years of LUE results and the above discussion, LUE shows considerable spatiotemporal variability, and the evergreen broad-leaved forest (EBF) ecosystem has the highest LUE, while the savanna ecosystem has the lowest. Therefore, it is maybe an alternative way to plant the EBF plantation to uptake CO_2 where water and temperature are favorable under the circumstance of global increasing CO_2 concentration and changing climate. Furthermore, the site-specific variation in determinants (e.g., P, T, VPD, PAR, and LAI) of LUE, especially the VPD and LAI, and the temporal dynamic of LUE should be considered carefully in LUE-based models when estimating GPP or predicting the carbon cycle, although similar/equal forest/vegetation types usually show nearly the same LUE. In the future, warming might well decrease LUE in the savanna ecosystem, while it may increase LUE in regions with abundant water and lower temperatures. However, our findings indicate that decreasing precipitation may reduce the LUE and GPP of forest ecosystems, especially savanna ecosystems.

Acknowledgments

We would like to acknowledge the staff and technicians of the Yuanjiang Research Station for Savanna Ecosystems; Xishuangbanna Station for Tropical Rainforest Ecosystem Studies; Ailaoshan Station for Subtropical Forest Ecosystem Studies; Public Technology Service Center of Xishuangbanna Tropical Botanical Garden, Chinese Academy of Sciences (CAS); Lijiang Forest Ecosystem Research Station, Kunming Institute of Botany, CAS; and all staff working at the above stations for their invaluable contributions to instrument maintenance, fieldwork and data collection. This study was supported by the Joint Foundation from the National Key Research and Development Program of China (2016YFC0502105); the National Natural Science Foundation of China and the Natural Science of the Yunnan Province (U1602234); the National Natural Science Foundation of China (NSFC) (31770528, 41671209, 41405143); Yunnan Natural Science Foundation of Yunnan Province, China (2015FB186); CAS-JSPS Cooperative Research Project (GJHZ1521); the CAS 135 project (2017XTBG-T01, 2017XTBG-F01); First-class disciplines construction project of Guizhou province (GNYL[2017]007); and the Chinese Academy of Sciences President's International Fellowship Initiative (2017VCA0036). Meteorological, eddy flux, and LAI data for three sites (YJ, XSBN, and ALS) can be found in the electronic supplement to this manuscript. More details on XSBN (BNS) are also available at AsiaFLUX

dataset (https://db.cger.nies.go.jp/asiafluxdb/?page_id=16). Unfortunately, third-party data from site LJ is restricted from access by our data application and usage agreement with Kunming Institute of Botany, CAS (KIB, CAS), which is not willing to share publicly now because of carbon/water flux/cycle related results or researches are still not published, and LJ's associated data are only available directly from KIB, CAS. Readers who interested in LJ's data should make sure to abide by the data usage agreement of KIB, CAS and must apply for the data permission by apply it from the site's principal investigator (Kun Xu, xukun@mail.kib.ac.cn) firstly and then access to these data through this link (https://figshare.com/s/c8612571e027b4a80de2). We gratefully acknowledge the support from PIs of the other three sites for sharing their data: XSBN: Yi-Ping Zhang, yipingzh@xtbg.ac.cn; ALS: Yi-Ping Zhang, yipingzh@xtbg.ac.cn; YJ: Qi-Hai Song, sqh@xtbg.ac.cn.

References

Alton, P. B., P. R. North, and S. O. Los (2007), The impact of diffuse sunlight on canopy light-use efficiency, gross photosynthetic product and net ecosystem exchange in three forest biomes, *Global Change Biology*, *13*(4), 776-787, doi:10.1111/j.1365-2486.2007.01316.x.

Aubinet, M., B. Chermanne, M. Vandenhaute, B. Longdoz, M. Yernaux, and E. Laitat (2001), Long term carbon dioxide exchange above a mixed forest in the Belgian Ardennes, *Agricultural and Forest Meteorology*, *108*(4), 293-315, doi:Doi 10.1016/S0168-1923(01)00244-1.

Austin, R. B., G. Kingston, P. C. Longden, and P. A. Donovan (1978), Gross energy yields and the support energy requirements for the production of sugar from beet and cane: A study of four production areas, *Journal of Agricultural Science*, *91*(3), 667-675.

Baldocchi, D. (2008), Breathing of the terrestrial biosphere: lessons learned from a global network of carbon dioxide flux measurement systems, *Australian Journal of Botany*, *56*(1), 1-26, doi:10.1071/Bt07151.

Baldocchi, D., H. S. Chu, and M. Reichstein (2018), Inter-annual variability of net and gross ecosystem carbon fluxes: A review, *Agricultural and Forest Meteorology*, *249*, 520-533, doi:10.1016/j.agrformet.2017.05.015.

Baldocchi, D., et al. (2001), FLUXNET: A new tool to study the temporal and spatial variability of ecosystem-scale carbon dioxide, water vapor, and energy flux densities, *Bulletin of the American Meteorological Society*, *82*(11), 2415-2434, doi:Doi 10.1175/1520-0477(2001)082.

Baldocchi, D., R. Valentini, S. Running, W. Oechel, and R. Dahlman (1996), Strategies for measuring and modelling carbon dioxide and water vapour fluxes over terrestrial ecosystems, *Global Change Biology*, *2*(3), 159-168, doi:DOI 10.1111/j.1365-2486.1996.tb00069.x.

Baldocchi, D. D. (2003), Assessing the eddy covariance technique for evaluating carbon dioxide exchange rates of ecosystems: past, present and future, *Global Change Biology*, *9*(4), 479-492, doi:DOI 10.1046/j.1365-2486.2003.00629.x.

Beer, C., et al. (2009), Temporal and among-site variability of inherent water use efficiency at the ecosystem level, *Global Biogeochemical Cycles*, *23*(2), doi:10.1029/2008gb003233.

Cannell, M. G. R., R. Milne, L. J. Sheppard, and M. H. Unsworth (1987), Radiation Interception and Productivity of Willow, *Journal of Applied Ecology*, *24*(1), 261-278, doi:Doi 10.2307/2403803.

Cao, M., X. Zou, M. Warren, and H. Zhu (2006), Tropical Forests of Xishuangbanna, China, *Biotropica*, *38*(3), 306-309.

Chan, O. C., X. Yang, Y. Fu, Z. Feng, L. Sha, P. Casper, and X. Zou (2006), 16S rRNA gene analyses of bacterial community structures in the soils of evergreen broad-leaved forests in south-west China, *FEMS Microbiol Ecol*, *58*(2), 247-259, doi:10.1111/j.1574-6941.2006.00156.x.

Cooper, J. P. (1970), Potencial production and energy conversion in temperate and tropical grasses, *Herbage Abstracts*, *40*(1), 1-13.

Eamus, D., L. B. Hutley, and A. P. O'Grady (2001), Daily and seasonal patterns of carbon and water fluxes above a north Australian savanna, *Tree Physiol*, *21*(12-13), 977-988.

Falge, E., et al. (2001), Gap filling strategies for defensible annual sums of net ecosystem exchange, *Agricultural and Forest Meteorology*, *107*(1), 43-69, doi:Doi 10.1016/S0168-1923(00)00225-2.

Fei, X.-H., et al. (2017), Eddy covariance and biometric measurements show that a savanna ecosystem in Southwest China is a carbon sink, *Scientific reports*, *7*(41025), doi: 10.1038/srep41025, doi:10.1038/srep41025.

Fei, X.-H., et al. (2018), Carbon exchanges and their responses to temperature and precipitation in forest ecosystems in Yunnan, Southwest China, *Science of The Total Environment*, *616-617*, 824-840, doi:10.1016/j.scitotenv.2017.10.239.

Fox, J., Z. Nie, J. Byrnes, M. Culbertson, S. DebRoy, M. Friendly, B. Goodrich, R. H. Jones, Adam Kramer, and G. Monette (2016), sem: Structural Equation Models, *R package version 3.1-8. https://CRAN.R-project.org/package=sem*.

Garbulsky, M. F., J. Penuelas, D. Papale, J. Ardo, M. L. Goulden, G. Kiely, A. D. Richardson, E. Rotenberg, E. M. Veenendaal, and I. Filella (2010), Patterns and controls of the variability of radiation use efficiency and primary productivity across terrestrial ecosystems, *Global Ecology and Biogeography*, *19*(2), 253-267, doi:10.1111/j.1466-8238.2009.00504.x.

Gilmanov, T. G., et al. (2010), Productivity, Respiration, and Light-Response Parameters of World Grassland and Agroecosystems Derived From Flux-Tower Measurements, *Rangeland Ecology & Management*, *63*(1), 16-39, doi:10.2111/Rem-D-09-00072.1.

Gilmanov, T. G., et al. (2007), Partitioning European grassland net ecosystem CO2 exchange into gross primary productivity and ecosystem respiration using light response function analysis, *Agriculture Ecosystems & Environment*, *121*(1-2), 93-120, doi:10.1016/j.agee.2006.12.008.

Gitelson, A. A., and J. A. Gamon (2015), The need for a common basis for defining light-use efficiency: Implications for productivity estimation, *Remote Sensing of Environment*, *156*, 196-201, doi:10.1016/j.rse.2014.09.017.

Grace, J. B., and K. A. Bollen (2005), Interpreting the Results from Multiple Regression and Structural Equation Models, *The Bulletin of the Ecological Society of America*, *86*(4), 283-295.

Green, D. S., J. E. Erickson, and E. L. Kruger (2003), Foliar morphology and canopy nitrogen as predictors of light-use efficiency in terrestrial vegetation, *Agricultural and Forest Meteorology*, *115*(3-4), 163-171.

Hall, F. G., K. F. Huemmrich, S. J. Goetz, P. J. Sellers, and J. E. Nickeson (1992), Satellite Remote-Sensing of Surface-Energy Balance - Success, Failures, and Unresolved Issues in Fife, *J. Geophys. Res.-Atmos.*, *97*(D17), 19061-19089, doi:Doi 10.1029/92jd02189.

He, H. L., et al. (2014), Large-scale estimation and uncertainty analysis of gross primary production in Tibetan alpine grasslands, *J. Geophys. Res.-Biogeosci.*, *119*(3), 466-486, doi:10.1002/2013jg002449.

Hollinger, D. Y., F. M. Kelliher, J. N. Byers, J. E. Hunt, T. M. Mcseveny, and P. L. Weir (1994), Carbon-Dioxide Exchange between an Undisturbed Old-Growth Temperate Forest and the Atmosphere, *Ecology*, *75*(1), 134-150, doi:Doi 10.2307/1939390.

Huang, H., Z. Chen, D. Liu, G. He, R. He, D. Li, and K. Xu (2017), Species composition and community structure of the Yulongxueshan (Jade Dragon Snow Mountains) forest dynamics plot in the cold temperate spruce-fir forest, Southwest China, *Biodiversity Science*, *25*(3), 255-264, doi:10.17520/biods.2016274.

Jia, W., M. Liu, Q. She, C. Yin, X. Zhu, and W. Xiang (2016), Optimization and evaluation of key photosynthesis parameters in forest ecosystems based on FLUXNET data and VPM model, *Chinese Journal of Applied Ecology*, *27*(4), 1095-1102.

Kanniah, K. D., J. Beringer, and L. B. Hutley (2011), Environmental controls on the spatial variability of savanna productivity in the Northern Territory, Australia, *Agricultural and Forest Meteorology*, *151*(11), 1429-1439, doi:10.1016/j.agrformet.2011.06.009.

Larcher, W. (2003), *Physiological plant ecology: ecophysiology and stress physiology of functional groups*, 4 ed., 513 pp., Springer Science & Business Media, Berlin, Germany.

Lee, X., W. Massman, and B. Law (2006), *Handbook of micrometeorology- A Guide for Surface Flux Measurement and Analysis*, Springer Science Business Media, New York.

Lee, X., and W. J. Massman (2010), A Perspective on Thirty Years of the Webb, Pearman and Leuning Density Corrections, *Boundary-Layer Meteorology*, *139*(1), 37-59, doi:10.1007/s10546-010-9575-z.

Li, C. C. (1975), *Path analysis-a primer*, The Boxwood Press.

Li, S. G., W. Eugster, J. Asanuma, A. Kotani, G. Davaa, D. Oyunbaatar, and M. Sugita (2008), Response of gross ecosystem productivity, light use efficiency, and water use efficiency of Mongolian steppe to seasonal variations in soil moisture, *J. Geophys. Res.-Biogeosci.*, *113*(G1), doi:10.1029/2006JG000349, doi:10.1029/2006jg000349.

Liu, F. Y., H. Zhu, J. P. Shi, and X. M. Chen (2007), Characteristics of plant communities and their soil fertilities in dry-hot valley of Yuanjiang County, Yunnan, China, *Chinese Journal of Applied and Environmental Biology*, *13*(6), 782-787.

Lloyd, J., and J. A. Taylor (1994), On the Temperature-Dependence of Soil Respiration, *Functional Ecology*, *8*(3), 315-323, doi:Doi 10.2307/2389824.

Mercado, L. M., N. Bellouin, S. Sitch, O. Boucher, C. Huntingford, M. Wild, and P. M. Cox (2009), Impact of changes in diffuse radiation on the global land carbon sink, *Nature*, *458*(7241), 1014-1017, doi:10.1038/nature07949.

Monteith, J. L. (1972), Solar-Radiation and Productivity in Tropical Ecosystems, *Journal of Applied Ecology*, *9*(3), 747-766, doi:Doi 10.2307/2401901.

Nichol, C. J., K. F. Huemmrich, T. A. Black, P. G. Jarvis, C. L. Walthall, J. Grace, and F. G. Hall (2000), Remote sensing of photosynthetic-light-use efficiency of boreal forest, *Agricultural and Forest Meteorology*, *101*(2-3), 131-142, doi:Doi 10.1016/S0168-1923(99)00167-7.

Nizami, S. M., Z. Yiping, Z. Zheng, L. Zhiyun, Y. Guoping, and S. Liqing (2017), Evaluation of forest structure, biomass and carbon sequestration in subtropical pristine forests of SW China, *Environ Sci Pollut Res Int*, *24*(9), 8137-8146, doi:10.1007/s11356-017-8506-7.

Odum, E. P., and G. W. Barrett (1971), *Fundamentals of ecology*, 574 pp., Saunders, Philadelphia, PA, USA.

Pangle, L., J. M. Vose, and R. O. Teskey (2009), Radiation use efficiency in adjacent hardwood and pine forests in the southern Appalachians, *Forest Ecology and Management*, *257*(3), 1034-1042, doi:10.1016/j.foreco.2008.11.004.

Piao, S., J. Fang, P. Ciais, P. Peylin, Y. Huang, S. Sitch, and T. Wang (2009), The carbon balance of terrestrial ecosystems in China, *Nature*, *458*(7241), 1009-1013, doi:10.1038/nature07944.

Potter, C. S., J. T. Randerson, C. B. Field, P. A. Matson, P. M. Vitousek, H. A. Mooney, and S. A. Klooster (1993), Terrestrial Ecosystem Production - a Process Model-Based on Global Satellite and Surface Data, *Global Biogeochemical Cycles*, *7*(4), 811-841, doi:Doi 10.1029/93gb02725.

Prince, S. D., and S. N. Goward (1995), Global primary production: A remote sensing approach, *Journal of Biogeography*, *22*(4-5), 815-835, doi:Doi 10.2307/2845983.

Qiao, N., D. Schaefer, E. Blagodatskaya, X. Zou, X. Xu, and Y. Kuzyakov (2014), Labile carbon retention compensates for CO2 released by priming in forest soils, *Glob Chang Biol*, *20*(6), 1943-1954, doi:10.1111/gcb.12458.

Qing, L. (2004), Effects of gap size and with-in gap position on the survival and growth of naturally regenerated Picea likiangensis seedlings, *Chinese Journal of Applied and Environmental Biology*, *10*(3), 281-285.

Reichstein, M., et al. (2005), On the separation of net ecosystem exchange into assimilation and ecosystem respiration: review and improved algorithm, *Global Change Biology*, *11*(9), 1424-1439, doi:10.1111/j.1365-2486.2005.001002.x.

Reichstein, M., et al. (2007), Determinants of terrestrial ecosystem carbon balance inferred from European eddy covariance flux sites, *Geophysical Research Letters*, *34*(1), L01402, doi:01410.01029/02006GL027880, doi:10.1029/2006gl027880.

Ruimy, A., P. Jarvis, D. Baldocchi, and B. Saugier (1995), CO2 fluxes over plant canopies and solar radiation: a review, *Advances in ecological research*, *26*, 1-68.

Running, S. W., R. R. Nemani, F. A. Heinsch, M. S. Zhao, M. Reeves, and H. Hashimoto (2004), A continuous satellite-derived measure of global terrestrial primary production, *Bioscience*, *54*(6), 547-560, doi:Doi 10.1641/0006-3568(2004)054[0547:Acsmog]2.0.Co;2.

Schemske, D. W., and C. C. Horvitz (1988), Plant-Animal Interactions and Fruit Production in a Neotropical Herb: A Path Analysis, *Ecology*, *69*(4), 1128-1137, doi:10.2307/1941267.

Schwalm, C. R., et al. (2006), Photosynthetic light use efficiency of three biomes across an east–west continental-scale transect in Canada, *Agricultural and Forest Meteorology*, *140*(1-4), 269-286, doi:10.1016/j.agrformet.2006.06.010.

Shi, H., L. H. Li, D. Eamus, J. Cleverly, A. Huete, J. Beringer, Q. Yu, E. Van Gorsel, and L. Hutley (2014), Intrinsic climate dependency of ecosystem light and water-use-efficiencies across Australian biomes, *Environmental Research Letters*, *9*(10), 104002, doi:10.1088/1748-9326/9/10/104002.

Song, Q.-H., X.-H. Fei, Y.-P. Zhang, L.-Q. Sha, C.-S. Wu, Z.-Y. Lu, K. Luo, W.-J. Zhou, Y.-T. Liu, and J.-B. Gao (2017), Snow damage strongly reduces the strength of the carbon sink in a primary subtropical evergreen broadleaved forest, *Environmental Research Letters*, *12*(10), doi:10.1088/1748-9326/aa82c4.

Still, C. J., J. T. Randerson, and I. Y. Fung (2004), Large-scale plant light-use efficiency inferred from the seasonal cycle of atmospheric CO(2), *Global Change Biology*, *10*(8), 1240-1252, doi:10.1111/j.1365-2486.2004.00802.x.

Tan, Z. H., Y. P. Zhang, D. Schaefer, G. R. Yu, N. S. Liang, and Q. H. Song (2011), An old-growth subtropical Asian evergreen forest as a large carbon sink, *Atmospheric Environment*, *45*(8), 1548-1554, doi:10.1016/j.atmosenv.2010.12.041.

Tan, Z. H., Y. P. Zhang, G. R. Yu, L. Q. Sha, J. W. Tang, X. B. Deng, and Q. H. Song (2010), Carbon balance of a primary tropical seasonal rain forest, *J. Geophys. Res.-Atmos.*, *115*, doi:10.1029/2009jd012913.

Tang, X., et al. (2018), Carbon pools in China's terrestrial ecosystems: New estimates based on an intensive field survey, *Proceedings of the National Academy of Sciences*, *115*(16), 4021-4026, doi:10.1073/pnas.1700291115.

Tang, X. G., H. P. Li, N. Huang, X. Y. Li, X. B. Xu, Z. Ding, and J. Xie (2015), A comprehensive assessment of MODIS-derived GPP for forest ecosystems using the site-level FLUXNET database, *Environmental Earth Sciences*, *74*(7), 5907-5918, doi:10.1007/s12665-015-4615-0.

Tanner, C. B., and G. W. Thurtell (1969), *Anemoclinometer measurements of Reynolds stress and heat transport in the atmospheric surface layer*, University of Wisconsin, Madison, Wisconsin.

Tong, X., J. Li, and Q. Yu (2009), Analysis of biophysical controls on light use efficiency in a farm land ecosystem, *Journal of Natural Resources*, *24*(8), 1393-1401.

Traore, A. K., P. Ciais, N. Vuichard, N. MacBean, C. Dardel, B. Poulter, S. Piao, J. B. Fisher, N. Viovy, and M. Jung (2014), 1982–2010 Trends of light use efficiency and inherent water use efficiency in African vegetation: sensitivity to climate and atmospheric CO2 concentrations, *Remote Sens-Basel*, *6*(9), 8923-8944.

Turner, D. P., S. Urbanski, D. Bremer, S. C. Wofsy, T. Meyers, S. T. Gower, and M. Gregory (2003), A cross-biome comparison of daily light use efficiency for gross primary production, *Global Change Biology*, *9*(3), 383-395, doi:DOI 10.1046/j.1365-2486.2003.00573.x.

Wang, X. C., C. K. Wang, and G. R. Yu (2008), Temporal and spatial patterns of forest carbon exchange based on global eddy fluxes, *Science in China Series D: Earth Sciences*, *38*(9), 1092-1102.

Webb, E. K., G. I. Pearman, and R. Leuning (1980), Correction of Flux Measurements for Density Effects Due to Heat and Water-Vapor Transfer, *Q J Roy Meteor Soc*, *106*(447), 85-100, doi:DOI 10.1002/qj.49710644707.

Wei, Y., and L. Wang (2010), The study on simulating light use efficiency of vegetation in Qinghai Province, *Acta Ecologica Sinica*, *30*(19), 5200-5216.

Wilczak, J. M., S. P. Oncley, and S. A. Stage (2001), Sonic anemometer tilt correction algorithms, *Boundary-Layer Meteorology*, *99*(1), 127-150, doi:Doi 10.1023/A:1018966204465.

Wootton, J. T. (1994), Predicting Direct and Indirect Effects - an Integrated Approach Using Experiments and Path-Analysis, *Ecology*, *75*(1), 151-165, doi:Doi 10.2307/1939391.

Wright, S. (1921), Correlation and causation, *Journal of agricultural research*, *20*(7), 557-585.

Wu, Z. Y., Y. C. Zhu, and H. Q. Jiang (1987), *Vegetation of Yunnan*, 508-510 pp., Science Press, Beijing.

Xiao, X. M. (2006), Light absorption by leaf chlorophyll and maximum light use efficiency, *Ieee T Geosci Remote*, *44*(7), 1933-1935, doi:10.1109/Tgrs.2006.874796.

Xiao, X. M., D. Hollinger, J. Aber, M. Goltz, E. A. Davidson, Q. Y. Zhang, and B. Moore (2004a), Satellite-based modeling of gross primary production in an evergreen needleleaf forest, *Remote Sensing of Environment*, *89*(4), 519-534, doi:10.1016/j.rse.2003.11.008.

Xiao, X. M., Q. Y. Zhang, B. Braswell, S. Urbanski, S. Boles, S. Wofsy, M. Berrien, and D. Ojima (2004b), Modeling gross primary production of temperate deciduous broadleaf forest using satellite images and climate data, *Remote Sensing of Environment*, *91*(2), 256-270, doi:10.1016/j.rse.2004.03.010.

Yebra, M., A. I. J. M. Van Dijk, R. Leuning, and J. P. Guerschman (2015), Global vegetation gross primary production estimation using satellite-derived light-use efficiency and canopy conductance, *Remote Sensing of Environment*, *163*, 206-216, doi:10.1016/j.rse.2015.03.016.

Yu, G. R., X. F. Wen, X. M. Sun, B. D. Tanner, X. H. Lee, and J. Y. Chen (2006), Overview of ChinaFLUX and evaluation of its eddy covariance measurement, *Agricultural and Forest Meteorology*, *137*(3-4), 125-137, doi:10.1016/j.agrformet.2006.02.011.

Yu, G. R., et al. (2013a), Spatial patterns and climate drivers of carbon fluxes in terrestrial ecosystems of China, *Glob Chang Biol*, *19*(3), 798-810, doi:10.1111/gcb.12079.

Yu, H. X., Z. J. He, and C. Q. Hong (2013b), Soil enzyme activity and its relationship with soil nutrient in the yulong snow mountain, *Journal of Yunnan Agricultural University*, *28*(5), 668-675.

Yuan, W., et al. (2014), Global comparison of light use efficiency models for simulating terrestrial vegetation gross primary production based on the LaThuile database, *Agricultural and Forest Meteorology*, *192-193*, 108-120, doi:10.1016/j.agrformet.2014.03.007.

Yuan, W. P., et al. (2007), Deriving a light use efficiency model from eddy covariance flux data for predicting daily gross primary production across biomes, *Agricultural and Forest Meteorology*, *143*(3-4), 189-207, doi:10.1016/j.agrformet.2006.12.001.

Zhang, L., P. Cao, Y. Zhu, Q. Li, J. Zhang, X. Wang, G. Dai, and J. Li (2015a), Dynamics and regulations of ecosystem light use efficiency in a broad-leaved Korean pine mixed forest, Changbai Mountain, *Chinese Journal of Plant Ecology*, *39*(12), 1156-1165.

Zhang, L. X., D. C. Zhou, J. W. Fan, and Z. M. Hu (2015b), Comparison of four light use efficiency models for estimating terrestrial gross primary production, *Ecological Modelling*, *300*, 30-39, doi:10.1016/j.ecolmodel.2015.01.001.

Zhao, M. S., F. A. Heinsch, R. R. Nemani, and S. W. Running (2005), Improvements of the MODIS terrestrial gross and net primary production global data set, *Remote Sensing of Environment*, *95*(2), 164-176, doi:10.1016/j.rse.2004.12.011.

Zhao, Y., S. Niu, J. Wang, H. Li, and g. Li (2007), Light use efficiency of vegetation: A review, *Chinese Journal of Ecology*, *26*(9), 1471-1477.

Zhou, Y. L., et al. (2016), Global parameterization and validation of a two-leaf light use efficiency model for predicting gross primary production across FLUXNET sites, *J. Geophys. Res.-Biogeosci.*, *121*(4), 1045-1072, doi:10.1002/2014jg002876.

Table 1

Table 1. Overview of the forest ecosystems (YJ, XSBN, ALS, and LJ) studied in the present research

	Research ecosystems			
Variables	**YJ**	**XSBN**	**ALS**	**LJ**
Ecosystem type	Savanna ecosystem	Tropical rainforest ecosystem	Subtropical evergreen broad-leaved forest ecosystem	Subalpine coniferous forest ecosystem
Geographical location	23°28′26″ N, 102°10′39″ E	21°55′39″ N, 101°15′55″ E	24°32′17″ N, 101°01′45″ E	27°08′32″ N, 100°13′38″ E
Altitude (m)	550	750	2500	3240
MAT (°C)	24.3	21.4	11.7	7.9
MAP (mm)	734	1415	1728	1095
Ratio of R/A	77%	80%	79%	80%
Soil type	Dry-red soil	Latosol	Yellow-brown soil	Dark-brown soil
Soil pH	7.3	4.5-5.5[b]	4.4-4.9[b]	5.6-5.9[d]
Organic carbon (g kg^{-1})	12.1	27.8[c]	138.4[c]	—
Total nitrogen (g kg^{-1})	1.0	2.8[c]	8.8[c]	4.0[e]
Total phosphorus (g kg^{-1})	0.30[a]	0.26[b]	0.82[b]	—
C/N ratio	12.1	9.9[b]	15.7[b]	—
Vegetation	Savanna	Tropical rainforest	Subtropical evergreen forest	Subalpine coniferous forest
Dominant species	*Lannea coromandelica, Polyalthia suberosa, Heteropogon contortus.*	*Terminalia myriocarpa, Barringtonia pendula, Saprosma ternatum, Pteris cretica.*	*Lithocarpus xylocarpus, Schima noronhae, Fargesia nitida, Plagiogyria communis.*	*Picea likiangensis, Abies forrestii, Quercus guayavifolia, Acer pectinatum, Padus brachypoda.*
Average canopy height (m)	4~6	35	25~30	38~42
LAI	~1.5	~5	~4.3	~3
Biomass (t ha^{-1})	~70[f]	>500[g]	~465.7[h]	—
Litterfall (t ha^{-1})	4.31[f]	9.91[g]	8.62[i]	5.11

Notes: MAT: mean annual temperature, MAP: mean annual precipitation; Ratio of R/A: the ratio of precipitation in rainy season to annual precipitation. References include the following: a [*Liu et al.*, 2007]; b [*Chan et al.*, 2006]; c [*Qiao et al.*, 2014]; d [*Qing*, 2004]; e [*Yu et al.*, 2013b]; f [*Fei et al.*, 2017]; g [*Tan et al.*, 2010]; h [*Nizami et al.*, 2017]; i [*Tan et al.*, 2011].

Table 2

Table 2. Instrumentation and variables measured in the studied forest ecosystems

Parameters	Ecosystems	Instruments and manufactures	Installed height (m)/ depth (cm)
Open-path eddy covariance system (OPEC)			
CO_2/H_2O concentration	YJ	Li-7500, Li-Cor, USA	13.9 m
	XSBN	Li-7500, Li-Cor, USA	48.8 m
	ALS	Li-7500, Li-Cor, USA	34.0 m
	LJ	Li-7500, Li-Cor, USA	60.0 m
Latent flux Sensitive flux Wind speed	YJ	WindMaster_1590 Gill, EN	13.9 m
	ALS	CSAT3, Campbell Sci, USA	34.0 m
	XSBN	CSAT3, Campbell Sci, USA	48.8 m
	LJ	CSAT3, Campbell Sci, USA	60.0 m
Routine meteorological observing system (RMOS)			
Air temperature Relative humidity	YJ	(HMP45, Vaisala, Helsinki, Finland)	2 layers (1.5, 13.5 m)
	XSBN		7 layers (4, 16, 26, 36, 42, 48.8, 69.8 m)
	ALS		7 layers (1.5, 4, 10, 18, 24, 30, 34 m)
	LJ		6 layers (1.5, 10, 20, 30, 40, 60 m)
Rainfall	YJ	(RainGauge 52203 Young, Traverse City, MI, USA)	13.9 m
	XSBN		72.0 m
	ALS		31.0 m
	LJ		60.0 m
Photosynthetically active radiation (PAR)	YJ	(LQS70-10, APOGEE, USA)	2 layers (1.5, 13.5 m)
	XSBN		6 layers (4, 10, 22, 31, 36, 70 m)
	ALS		6 layers (1.5, 4, 10, 18, 24, 30 m)
	LJ		1 layers (40 m)
Solar radiation	YJ	(CNR-1/CM11 Kipp & Zonen, Delft, the Netherlands)	8.5 m
	XSBN		41.0 m
	ALS		26.0 m
	LJ		50.0 m
Soil temperature	YJ	105T/107_L, Campbell, USA	5 layers (0, 5, 10, 20, 40 cm)
	XSBN		8 layers (0, 5, 10, 15, 20, 40, 60, 100 cm)
	ALS		8 layers (0, 5, 10, 15, 20, 40, 60, 100 cm)
	LJ		6 layers (0, 5, 10, 20, 40, 100 cm)
Soil volumetric water content	YJ	CS616_L, Campbell, USA	2 layers (5, 40 cm)
	XSBN		3 layers (5, 20, 40 cm)
	ALS		7 layers (5, 10, 20, 30, 40, 60, 100 cm)
	LJ		5 layers (5, 10, 20, 40, 100 cm)

Note: Data were available in YJ, XSBN, ALS, and LJ in May of 2013 to 2016, 2003 to 2016, 2009 to 2016 and in August of 2014 to 2016, respectively. Note that XSBN and ALS switched from the Li-7500 to the Li-7500A beginning in May 2014.

Table 3

Table 3. Eight-day binned LUE_{max} (g C · mol photon^{-1}) at annual time scale in the four studied forest ecosystems in Yunnan, Southwest China.

Year	YJ	XSBN	ALS	LJ
2003	—	0.650	—	—
2004	—	0.510	—	—
2005	—	0.560	—	—
2006	—	0.550	—	—
2007	—	0.650	—	—
2008	—	0.710	—	—
2009	—	0.520	0.678	—
2010	—	0.480	0.690	—
2011	—	0.380	0.691	—
2012	—	0.480	0.735	—
2013	0.169	0.430	0.827	—
2014	0.187	0.500	0.628	0.417
2015	0.172	0.610	—	0.491
2016	0.155	0.520	—	0.534
Average	**0.171**	**0.539**	**0.708**	**0.480**

Table 4

Table 4. Seasonal and annual variations in meteorological conditions in YJ, XSBN, ALS, and LJ, Southwest China.

Site	Period	Seasonal or annual sum			Seasonal or annual average			
		R_g	PAR	P	T_{air}	RH	SWVC	VPD
		MJ m^{-2}	mol m^{-2}	mm	°C	%	%	hPa
YJ	D	2918.7	5132.3	170.3	21.1	58.9	14.2	12.1
	W	3230.2	6337.5	563.6	27.7	63.4	16.6	15.2
	A	6148.9	11469.7	733.9	24.4	61.1	15.4	13.7
XSBN	D	2515.4	5150.2	288.6	18.8	75.9	17.8	6.6
	W	2647.4	5153.4	1124.9	24.0	82.4	23.4	6.0
	A	5162.9	10303.6	1413.5	21.4	79.1	20.6	6.3
ALS	D	2767.8	5077.3	307.9	9.0	66.9	30.2	4.4
	W	2261.7	4290.2	1321.3	14.3	86.9	34.5	2.4
	A	5029.5	9367.6	1679.2	11.7	76.9	32.3	3.4
LJ	D	2852.8	5595.7	219.5	4.2	54.9	26.8	4.2
	W	2345.8	4438.1	875.8	11.5	80.3	33.9	3.0
	A	5198.6	10033.7	1095.1	7.9	67.7	30.4	3.6

Note that D, W, and A indicate the dry season, the wet season, and annual values, respectively.

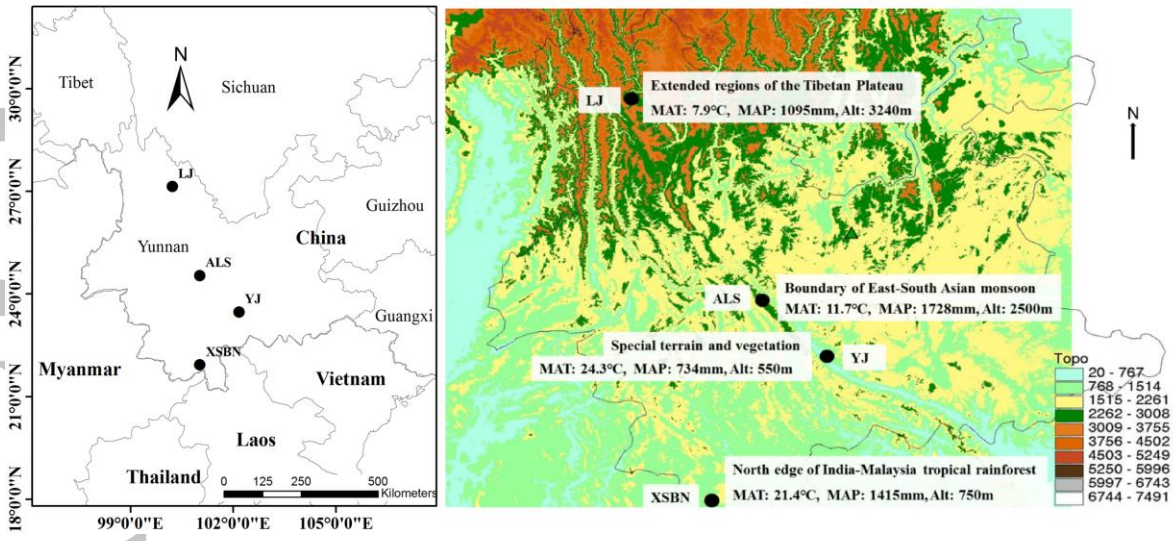

Figure 1. Geophysical location (a) and overview (b) of the studied ecosystems in Yunnan, Southwest China. Yuanjiang semiarid savanna ecosystem (YJ), Xishuangbanna tropical rainforest ecosystem (XSBN), Ailaoshan subtropical evergreen broad-leaved forest ecosystem (ALS), and Lijiang subalpine cold-temperate coniferous forest ecosystem (LJ). All the studied ecosystems are indicated by circles. MAT, MAP, and Alt represent the mean annual temperature, mean annual precipitation, and altitude, respectively.

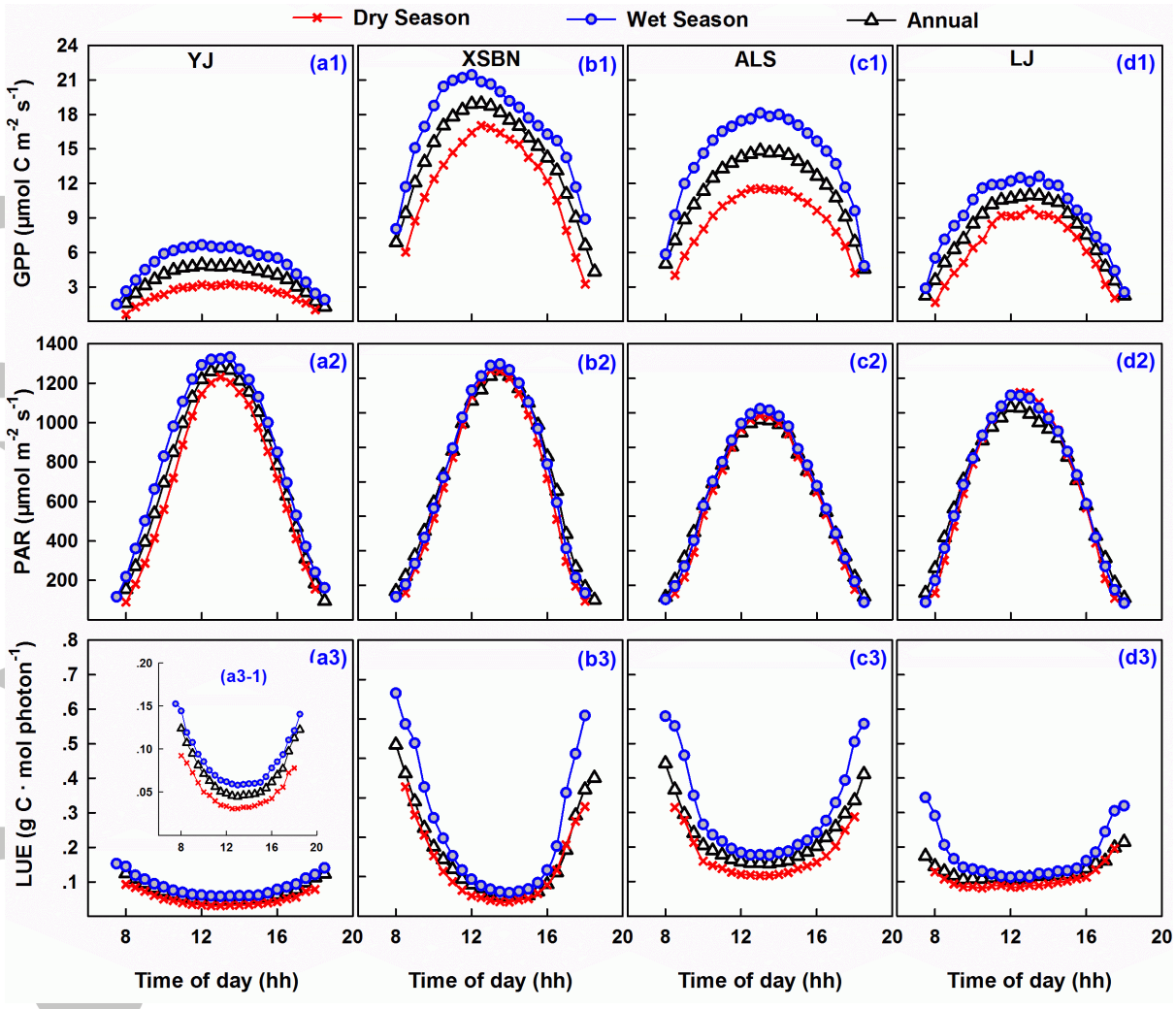

Figure 2. Seasonally and yearly averaged daytime trends of gross primary productivity (GPP), photosynthetically active radiation (PAR), and ecosystem light use efficiency (LUE) in YJ (a1-a3), XSBN (b1-b3), ALS (c1-c3), and LJ (d1-d3). Figure (a3-1) shows dramatic changes in the diurnal trends in LUE in YJ; the identical figure is shown in (a3), but the scale of the y-axis is different. The time of day is local time.

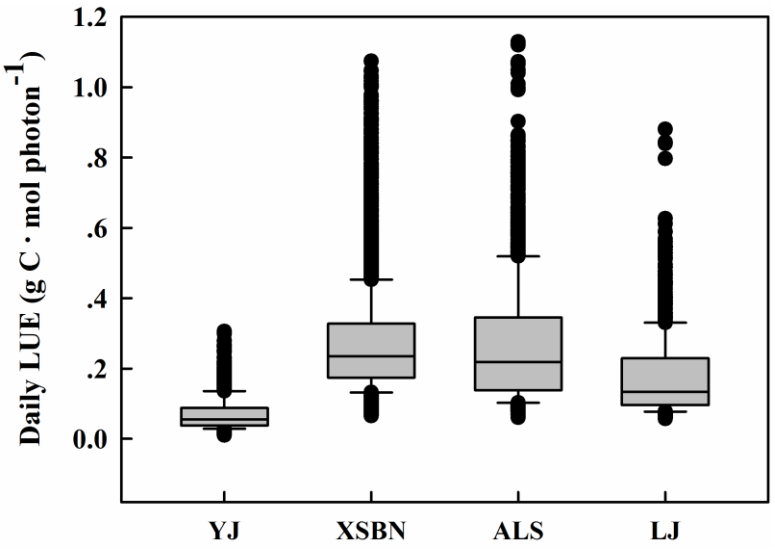

Figure 3. The range of daily LUE values during the study period in YJ, XSBN, ALS, and LJ. LUE values ranged from 0.008-0.316, 0.065-1.073, 0.060-1.129, and 0.052-0.881 g C · mol photon^{-1}, and the median value was 0.056, 0.235, 0.219, and 0.134 g C · mol photon^{-1} in YJ, XSBN, ALS, and LJ, respectively.

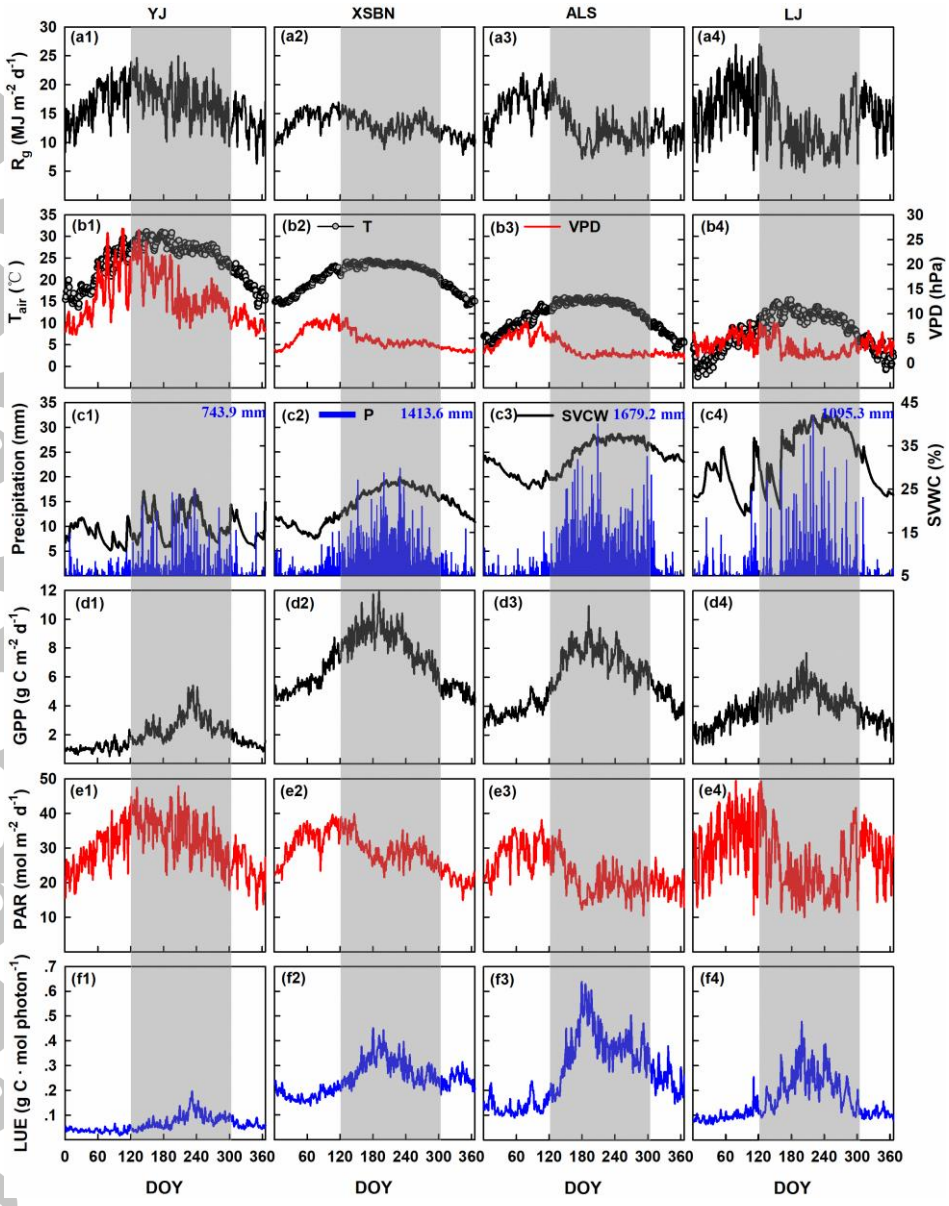

Figure 4. Intra-annual variations in controls and ecosystem light use efficiency (LUE) in Yuanjiang semiarid savanna ecosystem (YJ), Xishuangbanna tropical rainforest ecosystem (XSBN), Ailaoshan subtropical evergreen broad-leaved forest ecosystem (ALS) and Lijiang subalpine coniferous forest ecosystem (LJ), Yunnan Province, Southwest China. (a) Daily summed global radiation (R_g); (b) averaged daily air temperature (T_{air}, represented by gray-filled black circles) and saturation vapor pressure deficit (VPD, red lines); (c) soil volumetric water content (SVWC, black lines) at –5 cm depth and daily summed precipitation (Precipitation, blue-filled rectangle); (d) daily summed gross primary productivity (GPP); (e) daily summed photosynthetically active radiation (PAR); and (f) daily ecosystem light use efficiency (LUE). Shaded area indicates the wet season (May-October), and the remainder represents the dry season (November-April). Data were available in YJ, XSBN, ALS, and LJ in May of 2013 to 2016, 2003 to 2016, and 2009 to 2014, and in August of 2014 to 2016, respectively. All the data shown in this figure are multiday averaged values.

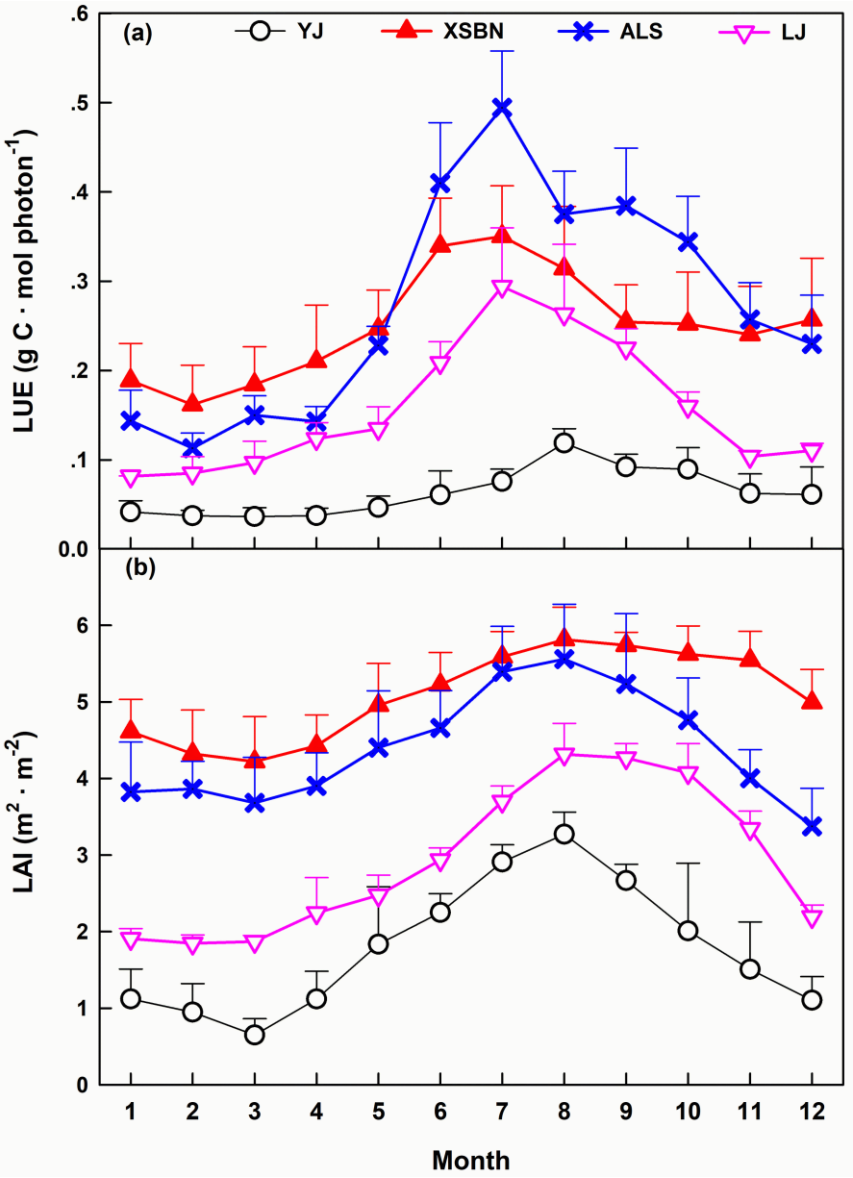

Figure 5. Monthly characteristics of (a) ecosystem light use efficiency (LUE) and (b) leaf area index (LAI) in the Yuanjiang semiarid savanna ecosystem (YJ), Xishuangbanna tropical rainforest ecosystem (XSBN), Ailaoshan subtropical evergreen broad-leaved forest ecosystem (ALS) and Lijiang subalpine coniferous forest ecosystem (LJ), Yunnan Province, Southwest China.

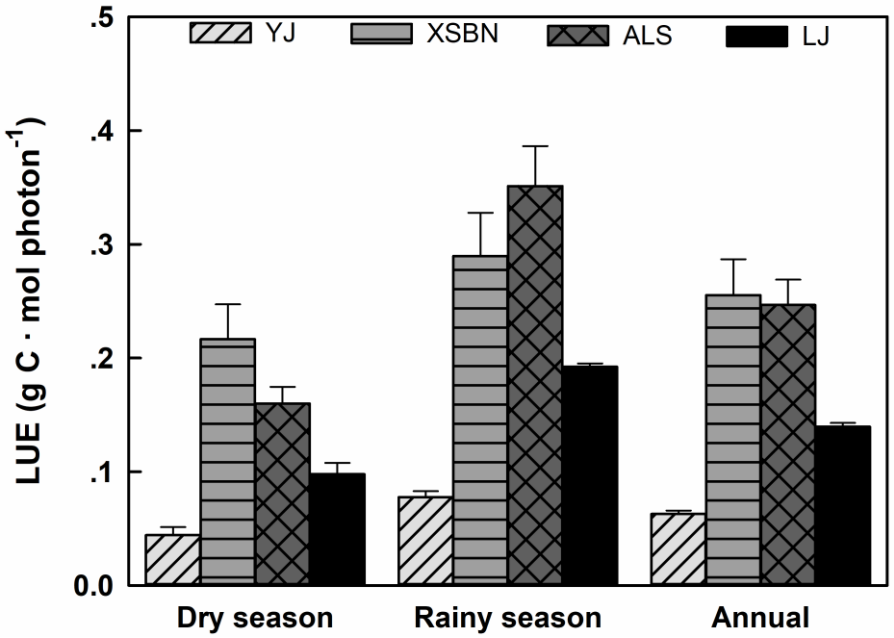

Figure 6. Seasonal and annual characteristics of ecosystem light use efficiency (LUE) in four contrasting forest ecosystems (YJ, XSBN, ALS, LJ), Yunnan Province, Southwest China.

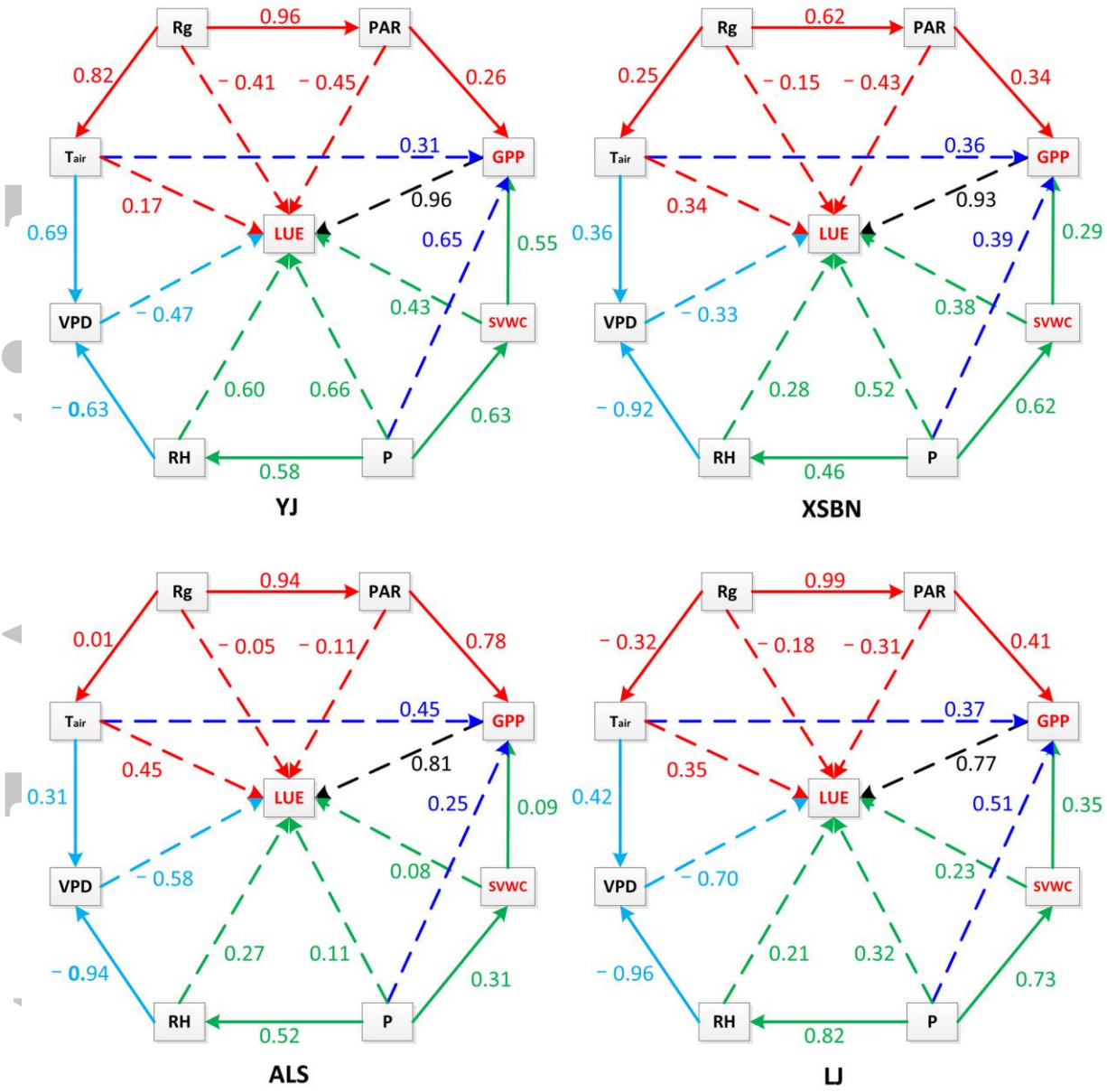

Figure 7. Schematic illustrating the effects of biophysical controls on monthly variations in LUE in typical forest ecosystems in Yunnan (YJ, XSBN, ALS, LJ). Solid arrows are direct effects (standardized partial regression coefficients), and dashed arrows indicate total effects (total effects = direct effects + indirect effects). The values adjacent to the solid arrows and dashed arrows represent the direct effect and the total effect, respectively. R_g, T_{air}, VPD, RH, P, SVWC, GPP and PAR indicate global radiation, air temperature, saturation vapor pressure deficit, relative humidity, precipitation, soil volumetric water content, gross primary productivity, and photosynthetically active radiation, respectively.

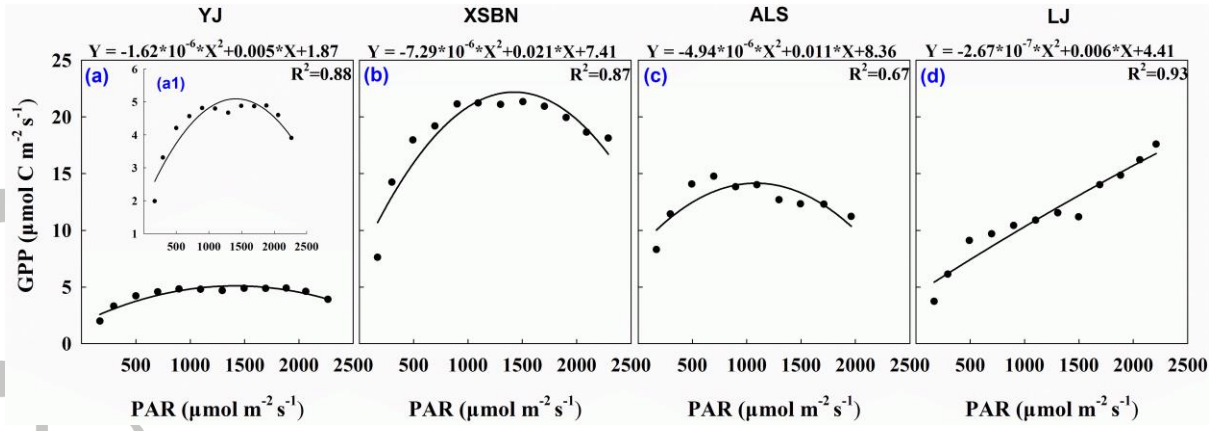

Figure 8. Light responses of GPP to binned PAR in Yunnan forest ecosystems (YJ, XSBN, ALS, and LJ). (a) Yuanjiang semiarid savanna ecosystem (YJ); (b) Xishuangbanna tropical rainforest ecosystem (XSBN); (c) Ailaoshan subtropical evergreen broad-leaved forest ecosystem (ALS); and (d) Lijiang subalpine coniferous forest ecosystem (LJ). Figure (a1), which shows the degree of sensitivity in the GPP response to PAR, shares the same dataset with (a), and the only difference is the scale of the y-axis.

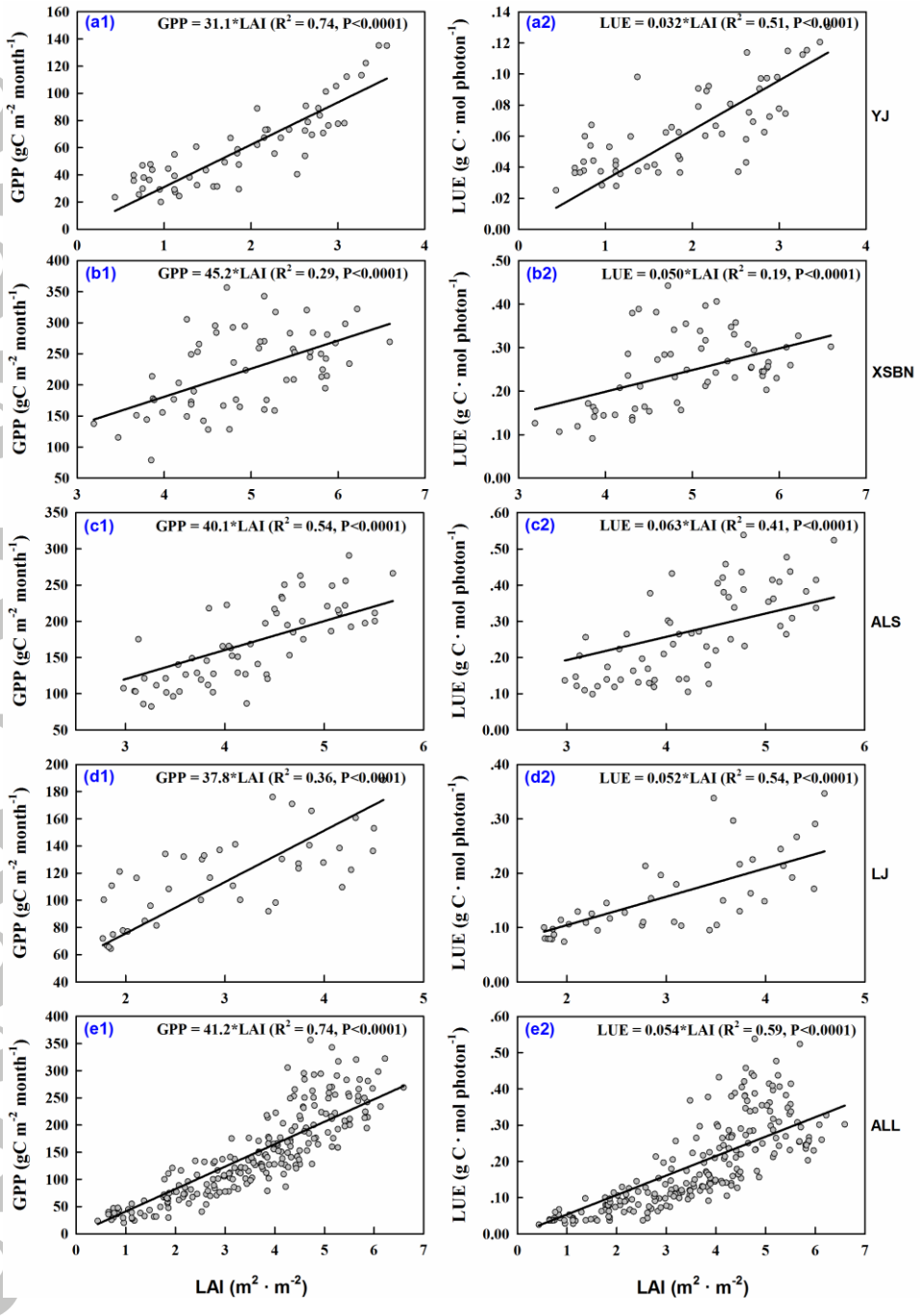

Figure 9. Influences of leaf area index (LAI) on gross primary productivity (GPP) and ecosystem light use efficiency (LUE) at a monthly scale. (a), (b), (c), and (d) represent YJ, XSBN, ALS, and LJ, respectively; (e) integrates all the studied forest ecosystems' GPP, LAI, and LUE values together correspondingly to explore how GPP and LUE respond to the variations in LAI in these forest ecosystems. The results indicated that LAI had a highly significant influence on the GPP and LUE in the studied forest ecosystems. In addition, Figure S2 in supplementary information reveals that the variation in yearly LAI dominated the dramatic change in LUE.

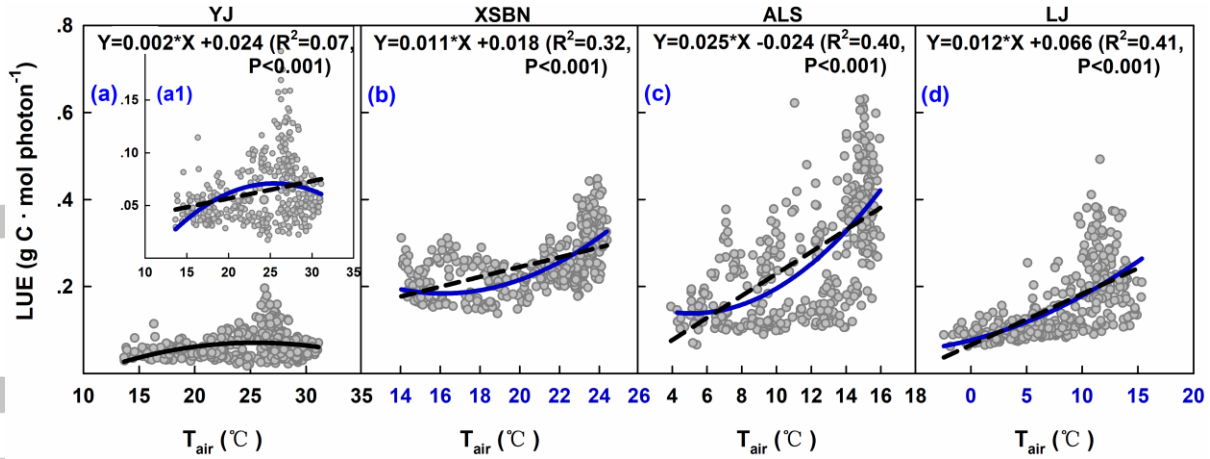

Figure 10. Linear/quadratic responses of ecosystem light use efficiency (LUE) to air temperature at daily timescales (n = 365) in Yunnan, Southwest China. (a) Yuanjiang semiarid savanna ecosystem, (b) Xishuangbanna tropical rainforest ecosystem, (c) Ailaoshan subtropical evergreen broad-leaved forest ecosystem, and (d) Lijiang subalpine coniferous forest ecosystem. The quadratic regression equation for YJ was $Y = -0.0003*X^2 + 0.0159*X - 0.131$ ($R^2 = 0.12$, $P < 0.001$), which suggested that warming will decrease LUE in the savanna ecosystem.

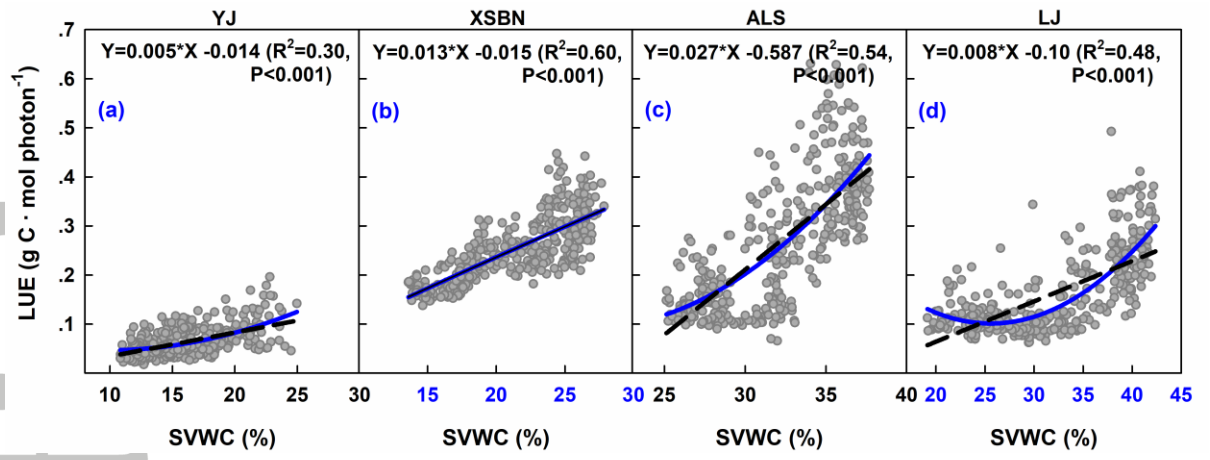

Figure 11. Linear/quadratic responses of ecosystem light use efficiency (LUE) to soil volumetric water content (SVWC) at daily timescales (n = 365) in Yunnan, Southwest China. (a) Yuanjiang semiarid savanna ecosystem, (b) Xishuangbanna tropical rainforest ecosystem, (c) Ailaoshan subtropical evergreen broad-leaved forest ecosystem, and (d) Lijiang subalpine coniferous forest ecosystem.